CHALMERS

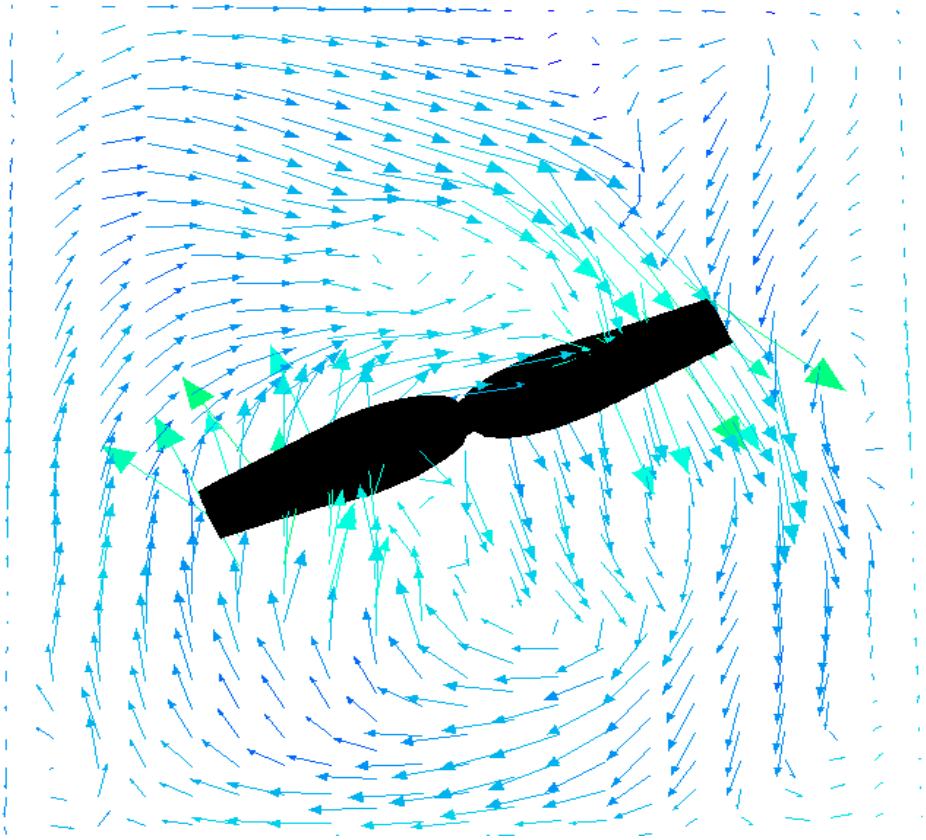

Numerical modelling and experimental investigations of a flocculation unit at Överby drinking water treatment plant

Master of Science Thesis in Infrastructure and Environmental Engineering

MOHAMED ISMAIL JAMA

Department of Civil and Environmental Engineering
Division of Water and Environmental Technology (WET)
CHALMERS UNIVERSITY OF TECHNOLOGY
Gothenburg, Sweden, 2013
Report No. 2013:150

Master thesis 2013:150

Numerical modelling and experimental investigations of a flocculation unit at Överby drinking water treatment plant

Master of Science Thesis in Infrastructure and Environmental engineering

MOHAMED ISMAIL JAMA

Department of Civil and Environmental Engineering
Division of Water and Environmental Technology (WET)
CHALMERS UNIVERSITY OF TECHNOLOGY
Gothenburg, Sweden, 2013

Numerical modelling and experimental investigations of a flocculation unit at Överby drinking water treatment plant

Master of Science Thesis in Infrastructure and Environmental Engineering
MOHAMED ISMAIL JAMA

Examensarbete/Institutionen för bygg- och miljöteknik
Chalmers Tekniska Högskola, 2013:150

Department of Civil and Environmental Engineering
Division of Water and Environmental Technology (WET)
Chalmers University of Technology
SE-412 96 Gothenburg, Sweden
Telephone: + 46 (0)31-772 1000

Cover:
The cover illustrates the modelled flow pattern for a specified section in the flocculation unit.

Chalmers Reproservice / Department of Civil and Environmental Engineering
Gothenburg, Sweden 2013

Numerical modelling and experimental investigations of a flocculation unit at Överby drinking water treatment plant

Master of Science Thesis in Infrastructure and Environmental Engineering

MOHAMED ISMAIL
Department of Civil and Environmental Engineering
Division of Water and Environmental Technology (WET)
Chalmers University of Technology

Abstract

The purpose of drinking water treatment plants (DWTPs) is to ensure that safe drinking water is provided to the consumers. Flocculation is one of the treatment processes in a DWTP and it is an important barrier. The understanding of the hydrodynamics in flocculation is therefore of great importance. In this project a flocculation unit in Överby DWTP has been modelled numerically. The velocity field obtained from the numerical model has been compared with experimental measured velocities in the flocculation unit. The velocity was measured with an Acoustic Doppler Velocimeter (ADV) instrument. The experimentally measured velocities and the numerically simulated flow pattern correlated fairly well. Additionally flow division calculations have been made to estimate how much water that goes to the new and old flocculation sections in the plant. The velocity measurements for the flow division calculations were made with a propeller type current meter. The flow division calculation gave lower flows than initially thought.

Keywords: CFD, flocculation unit, drinking water, sliding mesh, ADV

Table of Contents

1. Introduction

The availability of safe drinking water is essential for our society and it is important to minimize the risk of infection of waterborne diseases caused by drinking water. Consequently, raw water needs to be adequately treated prior being distributed to consumers. The drinking water treatment plant (DWTP) is constructed to ensure reliable, continuous and safe drinking water. DWTPs can look different in terms of which treatment processes they use. The treatment processes that are used are dependent on the initial raw water quality and the type of water that is treated; groundwater or surface waters (Crittenden et al. 2012). The conventional treatment processes for removing most constituents in the raw water are coagulation, flocculation, clarification (sedimentation), filtration and disinfection. In this report the flocculation step will be further investigated.

At the coagulation-flocculation step particles and colloids are destabilized by the addition of a coagulant. In the flocculation unit the destabilized particles are allowed to agglomerate into larger flocs to enhance settling in the clarification/sedimentation step (Crittenden et al. 2012). The flocculation step is one of the microbial barriers in a DWTP. The understanding of the floc scale physicochemical processes together with the hydrodynamics in a flocculation unit is of great importance. Previous research conducted by Samaras et al. (2010) has shown that the hydrodynamics in a flocculation unit can be modelled numerically for optimizing the flocculation treatment step. Furthermore it has been demonstrated in the study made by Zhao et al. (2013) and Li et al. (2006) that experimental measurements can be carried out to determine floc properties.

1.2 Aim and Objectives

The aim of this Master thesis is three-fold:

- To make a literature study on how flocculation units have been investigated previously by both experimental and modelling approaches.
- To set up a numerical model of a flocculation unit at the Överby DWTP and simulate the flow using ANSYS Fluent.
- To perform experimental measurements regarding flow velocity in the flocculation unit at the Överby DWTP.

1.3 Limitations

- Available computer power.
- Limited access to the flocculation units and channels at Överby DWTP.

2. Water treatment

In this chapter, an introduction to drinking water treatment and an overview on coagulation-flocculation is presented. In addition Överby drinking water treatment plant (DWTP) will be shortly described.

2.1 Water treatment

There exist numerous constituents in the raw water that needs to be eliminated in order to provide safe and aesthetic drinking water.The constituents existing in surface waters are mainly inorganic and organic particles, colloids, pathogens, and natural organic matter (NOM) mainly in form of fulvic and humic acids (Edzwald 1993). A DWTP is designed to treat raw water and to remove these constituents to an extent that safe drinking water can be provided to the consumers (Crittenden et al. 2012). The schematic outline of a conventional DWTP can be viewed in Figure 1. The first treatment process in a DWTP is usually coagulation-flocculation. At the coagulation-flocculation step particles and colloids are destabilized by the addition of a primary coagulant. In the flocculation unit the destabilized particles are allowed to agglomerate into larger flocs (Crittenden et al. 2012). A more in depth description of the coagulation-flocculation process can be read in Section 2.2. The consecutive step after the coagulation-flocculation is the clarification/sedimentation step. When the water enters the clarification basin(s) the created flocs from the previous step are allowed to settle from the main water column. The small flocs that do not settle are removed in subsequent granular filters; rapid sand filters, slow sand filters or a combination of these. The last treatment step in a conventional treatment plant is usually disinfection.

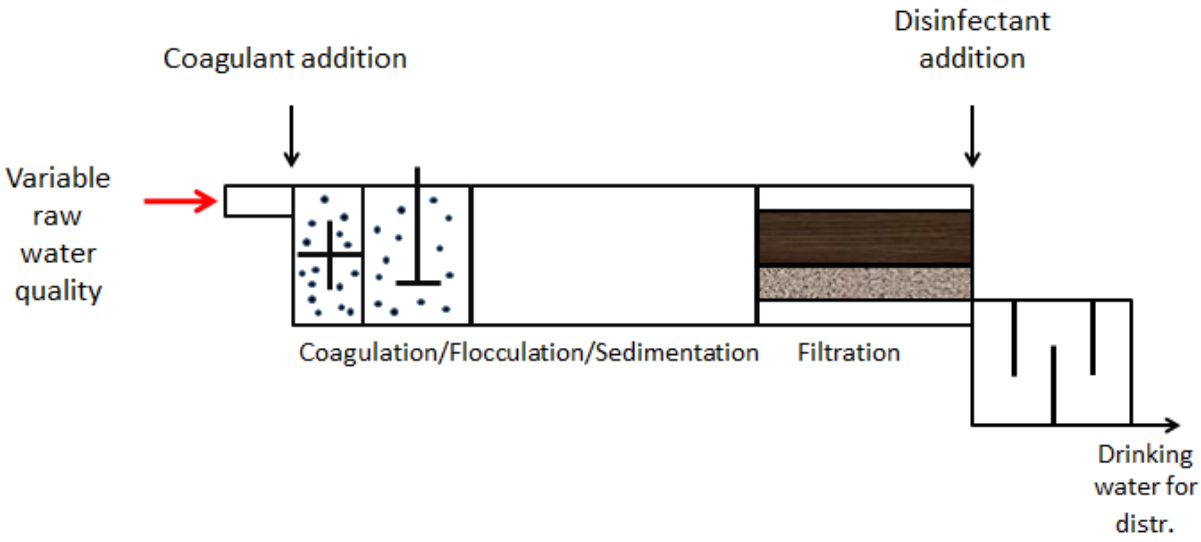

Figure 1. Schematic overview of treatment processes of raw water to fully treated drinking water in a conventional DWTP.

2.2 The coagulation-flocculation step

The coagulation step involves the addition of a primary coagulant and it is often in the form of metal salts or organic polymers (Betancourt & Rose 2004). In the coagulation step the coagulant can be mixed into the raw water by two mixing principles; hydraulic mixing or mechanical mixing (paddle-type stirrers or blade-type impeller stirrers) see Figure 2. In hydraulic mixing the mixing is generated by the walls (baffles) in the mixing-channel that induces sudden directional changes in the flow (Crittenden et al. 2012). Edzwald (2013) advocates mixing by hydraulic means at the coagulation step since energy savings can be made by the elimination of rapid mixers. At the flocculation step the aim is to achieve larger aggregates of particles called flocs by using one of the aforementioned mixing principles (Crittenden et al. 2012).

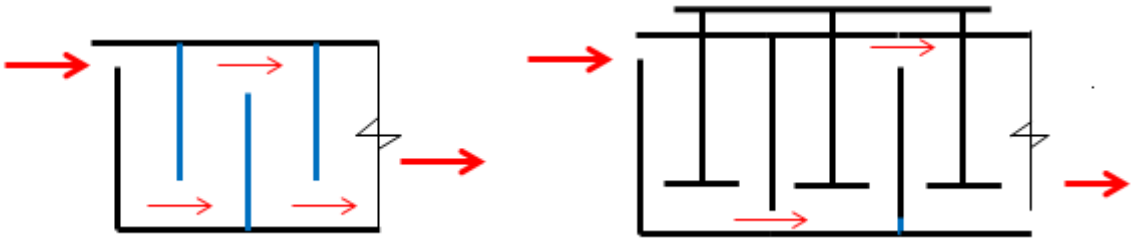

Figure 2. Hydraulic mixing channel with baffles (left) and mechanical blade-type impeller mixing (right).

At the coagulation step, the coagulant is rapidly mixed into the water to destabilize the particles and the colloids present in the water. Two main destabilization mechanisms of particles can be distinguished; *charge neutralization* and *sweep flocculation*. *Charge neutralization* occur when the pH <6 and positive metal species such as $Al(OH)^{+}$, $Al_8(OH)^{4+}$, and Al^{3+} are formed. Rapid mixing is crucial here to ensure that the metal species react with the particles and neutralize their negative surface charge prior hydroxide precipitation (Jiang & Graham 1998). *Sweep coagulation* on the other hand occurs when pH>6, alkalinity is prevalent and when higher doses of the coagulant is added. The predominant mechanism here is not the positively charged metal species but the formation and precipitation of metal hydroxide. These hydroxides acts like large clouds and “sweeps” particles and other soluble species in the bulk water phase. Generally, both these destabilization mechanisms occur although the more important mechanism is sweep coagulation (Jiang & Graham 1998).

The consecutive step in the treatment process is the flocculation. In the flocculation units the water is slowly mixed to reduce the risk of floc breakage and to ensure that larger aggregates of flocs with higher density are formed. The flocculation units that use mechanical mixing are configured in such a manner that the velocity of the impeller is decreased for each unit to minimize the risk of flock breakage as the flocs increase in size (Crittenden et al. 2012).

3. Experimental investigations

In this chapter previous experimental investigations made for flocculation hydrodynamics and floc scale physiochemical properties will be presented.

3.1 Experimental investigations on floc scale physiochemical properties

The importance of using the correct coagulant dose depending on the type of raw water being treated is stressed by Bunker et al. (1995). For instance, optimization of the coagulation step is suggested as a mean to improve removal of NOM (Matiliainen et al. 2010). The overdosing of a coagulant may increase the operating costs at the plant or pose a risk to public health. On the other hand, under-dosing the coagulant may decrease the efficiency of the plant and lead to insufficient removal of NOM and particulate matter Bouyer et al. (2001). The investigation of coagulant dose addition and its effect on floc characteristics is of importance.

Experimental investigations are often made to investigate the coagulation-flocculation step and the following floc-scale physiochemical parameters may be investigated; floc-strength, floc fractal dimension and floc size (Zhao et al. 2013).

3.1.1 Floc-strength dependency on coagulant dose

In a study made by Zhao et al. (2013) the increase of coagulant dose lead to a strong increase in floc-strength factor for ($Al_2(SO_4)_3$ but only up to the calculated optimal dose of 40 mg/l to later significantly decrease. For ($FeCl_3$) the floc-strength factor was fairly constant for all coagulant doses until it reached its coagulant dose optimum and increased. The ($TiCl_4$) showed little variation in floc-strength factor with an increase in coagulant dose however a minor decrease of floc-strength could be seen when dosed above its optimum dose.

3.1.2 Floc fractal dimension

The floc is sometimes described using the concept of floc fractal dimension (D_f). The floc D_f is a dimensionless number and a measurement of the “compactness” of a floc. Densely packed flocs have higher fractal dimension than loosely aggregated flocs. The D_f can for instance be estimated by the Small Angle Laser Light Scattering technique (SALLS) (Xu et al. 2012). In jar test experiments made by Li et al. (2006) the floc D_f was estimated when using $Al_2(SO_4)_3$ as a primary coagulant. For sweep coagulation the floc D_f could be estimated to be between 2.58 - 2.91. The floc D_f is usually between 1-3 (Li et al. 2006).

3.1.3 Floc size dependency on coagulant dose and induced shear rate

In the study made by Zhao et al. (2013) it was shown that an increase in coagulant dose above the optimal doses for the three coagulants Aluminium sulfate ($Al_2(SO_4)_3$), Ferric chloride ($FeCl_3$), and Titanium tetrachloride ($TiCl_4$) led to a decrease in floc size. This decrease in floc size is reasoned to be the result of overcharging of particles. It has previously been established that high coagulation doses might be more than enough for just neutralizing the surface charge of particles and instead give rise to positively charged particles that repel each other (Crittenden et al. 2012). Additionally, a decrease in pH with increased coagulant dose lead to dissolution of flocs (Zhao et al. 2013).

When it comes to the effect of induced shear rate on floc size the study by Zhao et al. (2013) has shown that with increased shear rates the floc size decreases. This phenomenon has also been demonstrated by Bouyer et al. (2001).

3.2 Particle image velocimetry (PIV)

The hydrodynamics of a flocculation unit can be experimentally investigated by scaling down the flocculation unit of interest and performing jar-tests (Bouyer et al. 2001). In a study made by Coufort et al. (2004) particle image velocimetri (PIV) was used to experimentally assess the hydrodynamics in flocculation. Since PIV is an image analysis tool the flocculation of particles can also be experimentally assessed. Data on floc area from the PIV can be used to calculate a floc distribution in the jar either with regards to flocs in numbers or floc size. The most probable floc number and/or the most probable floc size in the jar can then be estimated. In the study performed by Coufort et al. (2004) it was concluded that floc size is highly dependent on the velocity gradients created by the hydrodynamics. In the study made by Xiao et al. (2011) PIV is suggested as a robust imaging tool to experimentally evaluate the hydrodynamics and to experimentally assess the flocculation of particles. It was concluded from the study that flocs were largest and had highest D_f just after the addition of a primary coagulant. Further it could be seen when floc breakage occurred and re-flocculation took place the flocs showed only little recoverability of D_f.

The above investigations have demonstrated that using jar-tests are a valuable tool when evaluating the flocculation process. However, a study by Kilander et al. (2007) has shown that changes in dynamics of the flocculation may occur when scaling up the system.

4. Överby drinking water treatment plant

In this report, the flocculation section at Överby drinking water treatment plant (DWTP) will be of focus. Therefore, a short background on Överby DWTP treatment plant is presented here. The DWTP was constructed in 1962 and a capacity expansion was made between the years 1972-1974 due to an increase in water demand. The treatment plant provides fresh drinking water to approximately 49 000 inhabitants in the municipality of Trollhättan. The production capacity is 30 000 m^3/day, the mean production year 2012 was approximately 14 125 m^3/day.

The treatment plant is a conventional treatment plant. A schematic figure of the treatment processes in Överby DWTP can be viewed in Figure 3. The raw water is withdrawn from Göta Älv river. The water initially passes through large sieves to reduce the intermediate to large constituents in the water before the water is pumped into the treatment plant. In the plant carbon dioxide and slaked lime is added to increase hardness and alkalinity of the water prior to the addition of a primary coagulant. Polyaluminium chloride (PAX) is used as a primary coagulant and it is mixed into the water by hydraulic means. The plant has a new and an old flocculation section. The flow division between the two flocculation sections are believed to be 30 % and 70 % respectively. The new section employs paddle-type stirrers while the old section uses blade type-impeller stirrers. After the flocculation the water enters the sedimentation chambers. To eliminate flocs and fine particles that did not settle in the sedimentation chambers both rapid sand filters and slow sand filters are employed in the plant. Sodium hypochlorite (NaClO) is used as a disinfectant.

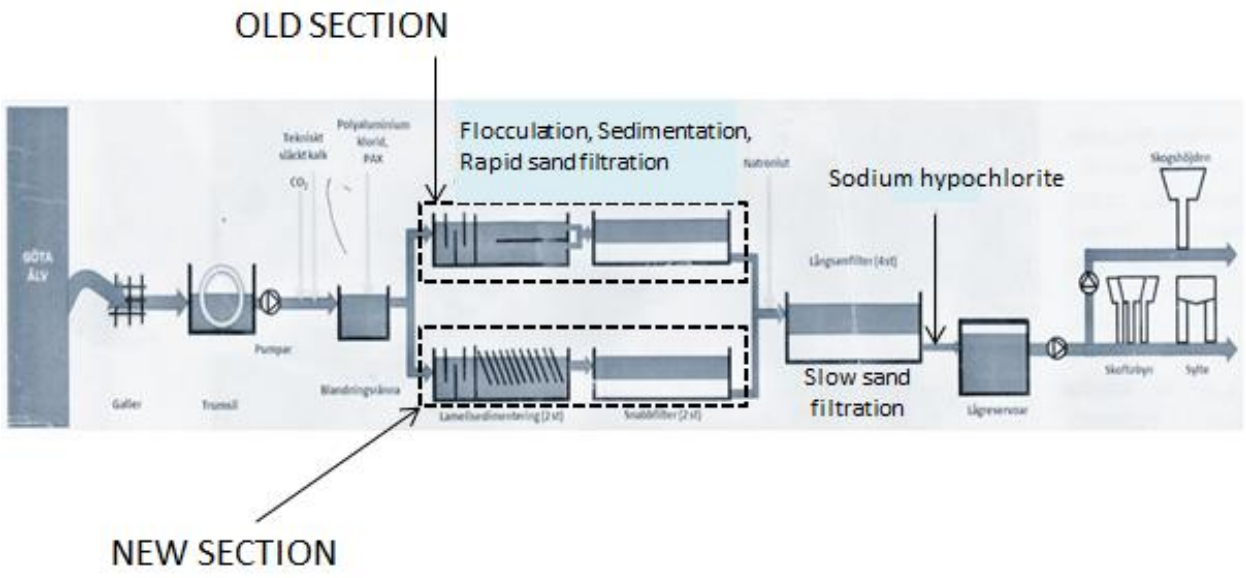

Figure 3. Schematic overview of the treatment processes employed in Överby DWTP from inlet to distribution (Trollhättan energi 2013).

5. Numerical investigations

The advantages of numerical investigations are that they can be carried out to capture the physics of large-scale processes when experimental investigations are not feasible for practical reasons. Flocculation units have been covered in previous studies but then mostly for other applications such as the mineral processing industry (Somasundaran et al. 2003). Many of the computational techniques used when modelling flocculation units are however similar and same procedures and methods can be employed when modelling flocculation units in drinking water treatment plants (DWTPs). In this chapter the steps of setting up a numerical model will be introduced and previous research on the topic will be covered.

5.1 Steps of setting up a numerical model

The method of setting up a numerical model is comprised of several steps. The steps are Pre-processing, Solving and Post-processing (Jiyuan et al. 2012).

5.1.1 Pre-processing

The Pre-processing step can be divided into two parts; the geometry generation and mesh generation. Most commercial CFD-codes have a CAD-software for the geometry generation and an integrated meshing programme for the mesh generation. Commonly, the geometry is supplied by the client and can be readily imported into the CAD-software. In many cases the CAD-geometry supplied is too detailed for the purpose of CFD simulations and simplifications of the geometry are then needed (Andersson 2011). When the geometry is set, it needs to be divided into small sub-volumes/cells where the governing fluid flow equations are solved. It is this division of the geometry into small sub-volumes that is referred to as the meshing generation.

5.1.2 Solving

In the Solving step the physics of the problem is set. For instance in the CFD-code ANSYS Fluent, the governing fluid flow equations are discretized by the finite volume method (FVM) and solved for each cell in the mesh. Further, the turbulent closure model suiTable for the specific case is chosen. Many parameters can be altered in this step, for example; the solver scheme, the discretization scheme, the number of iterations/time steps that are desired etc. Also, mesh refinement and adaptation for increased accuracy can be done. Monitoring parameters of interest during calculation can also be done in the solver (Jiyuan et al. 2012).

5.1.3 Post-processor

The Post-processor step is the last step in a CFD-simulation process. In this step the results from the simulation can be examined using for instance graphs, XY-plots, and contour plots.

5.2 Investigations on numerical modelling

Both small and full-scale flocculation units have been modelled previously and the work demonstrates that numerical modelling is an important tool in optimizing flocculation units (Samaras et al. 2010).

Bridgeman et al. (2009) made numerical models using the commercial CFD-program ANSYS Fluent for two jar-test set-ups representing small-scale flocculation units. The two jar-tests investigated had different geometrical shapes and configurations. The first jar-test flocculator was a cylindrical unbaffled flocculator with 100 mm in diameter and 127 mm in water depth. The second configuration consisted of a square shaped flocculator with sides of 115 mm in length and 150 mm in water depth. Both configurations had a paddle-type stirrer

in the centre with a diameter of 76 mm. For both flocculators two different modelling approaches for rotation were used in combination with six different turbulence models this to evaluate the most suiTable combination. The two evaluated approaches for modelling rotation were Multiple reference frames (MRF) and the more advanced Sliding mesh (SM) modelling approach. The turbulence models evaluated were Standard k-ε (Sk-ε), Realizable k-ε (rk-ε), Renormalized group k-ε (RNG k-ε), Standard k-ω (Sk-ω), Shear stress turbulence k-ω (SSTk-ω), and Reynolds stress model (RSM). The limit for scaled residuals for assessing convergence was set to $1x10^{-5}$. The axial velocity data obtained from the numerical models were compared with experimental velocity measurements carried out using a Laser Doppler Anemometry (LDA) instrument.

The flow field in a full-scale flocculation unit has been modelled by Samaras et al. (2010). Like Bridgeman et al. (2009), Samaras et al. (2010) discusses the importance of choosing the appropriate turbulence model and the method to model the rotational flow. The flocculation unit modelled by Samaras et al. (2010) was a cylindrical tank with dimensions 9570 mm in diameter at the bottom and 7560 mm in diameter at the top and 5650 mm in height. For the rotation a blade-type impeller was placed in tank centre with diameter 3880 mm. For setting up the numerical model the tank was divided into two parts; one inner rotational impeller region (rotor) and one outer stationary region (stator). In a case with a cylindrical tank geometry that has radial symmetry (e.g. no baffles, no square tank, no side inputs/outputs etc.) and where the rotation is created by an impeller with numerous blades the MRF modelling approach is valid (Samaras et al. 2010). The MRF technique of modelling rotation can be used even if the tank is not designed as having radial symmetry. It is then, however, important to evaluate the degree of interaction between the rotational region and those things that destroy the radial symmetry. Such evaluation can for instance be taking the ratio between the tank diameter/width and the impeller diameter (Samaras et al. 2010). In the work of Samaras et al. (2010) the use of the MRF technique of modelling was justified since weak interaction was shown between the water stream input at the boundaries of the tank and the rotation in the tank. Based on the study made by Bridgeman et al. (2009) the two-equation turbulence model RNG k-ε was chosen by Samaras et al. (2010) since it was shown to gives reasonable accurate results for the velocity distribution.

6. Method

The method chapter describes the geometry of the flocculation section in the plant. Further, the modelling strategies used as well as descriptions of experimental measurements are presented.

6.1 Geometry of the flocculation section

There are four parallel lines in the old flocculation section at Överby drinking water treatment plant (DWTP), Figure 4. The flocculation unit investigated is the flocculation unit number one located in the first flocculation line. At the end of the inlet channel the water is divided into two separate flows; flow Q3 to the new flocculation section and flow Q2 to the old flocculation section. Flocculation units 1-6 are interconnected and the water flows into flocculation unit number one from the distribution channel just outside. The water is passed through to flocculation unit number two. The water then continues to flow in similar fashion through the remaining flocculation and reaches the last flocculation unit. The water is discharged through the outlet channel to one of the sedimentation tanks see Figure 4.

From architectural blueprints provided by the treatment plant and measurements of the water level in the distribution channel the dimensions of the geometry could be estimated, Figure 5. The impeller dimensions were provided by the impeller manufacturer Sulzer.

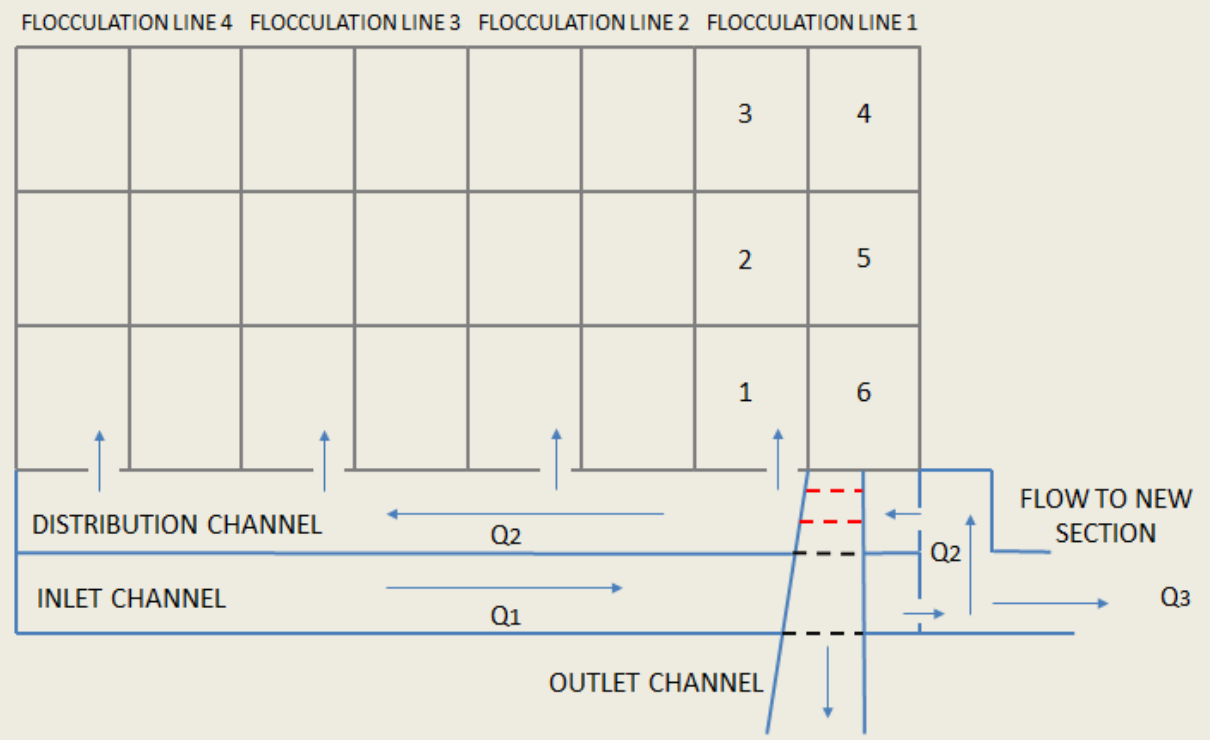

Figure 4. Schematic overview of the old flocculation section with its flocculation lines. The black dotted lines symbolize the water going under the outlet channel and the red dotted lines symbolize the tunnel through the outlet channel.

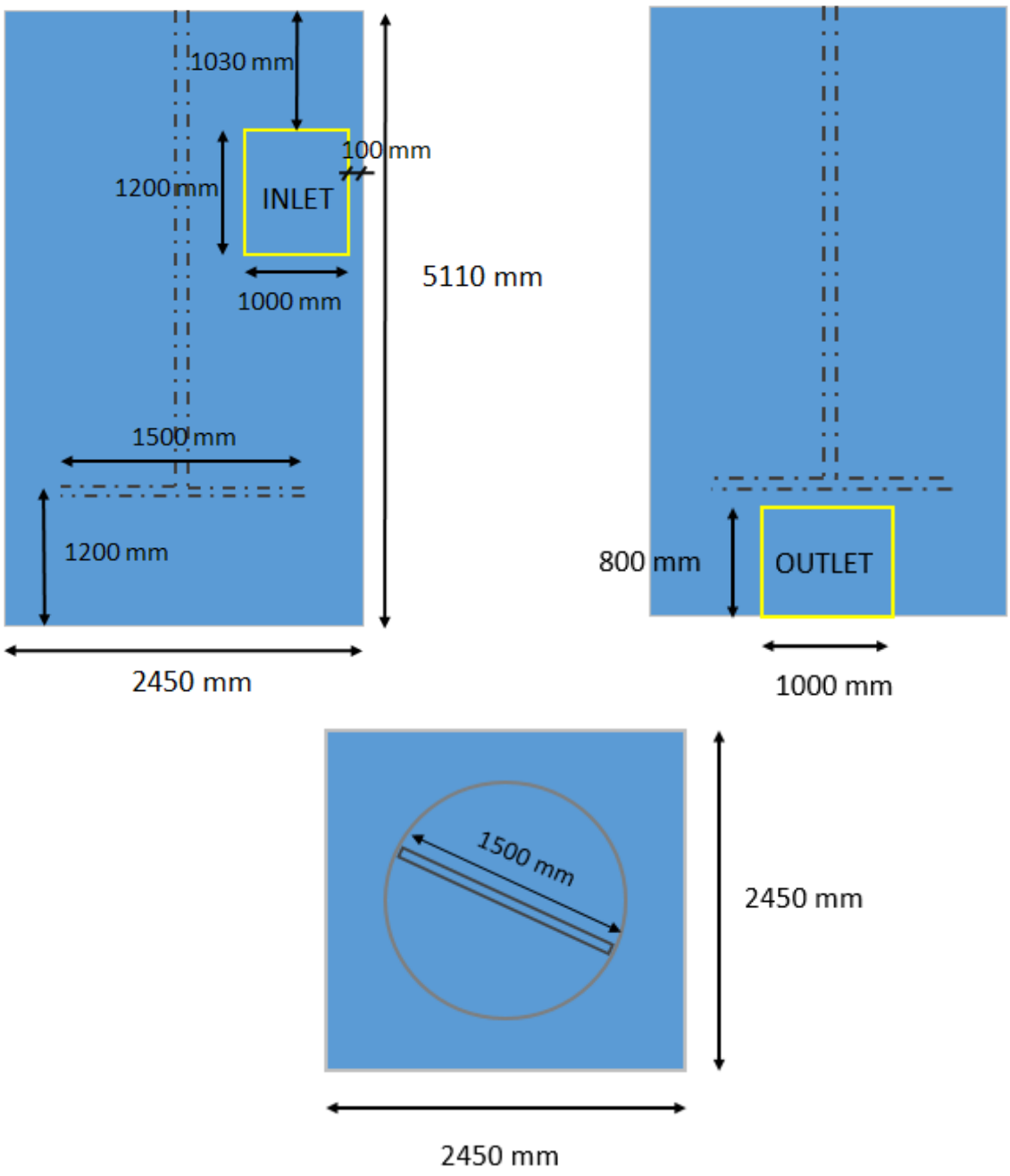

Figure 5. Dimensions of flocculation unit number one. *Top left*: front view of the unit. *Top right*: back view of the unit. *Bottom*: Top view of the unit where the cylindrical rotational region and impeller can be viewed.

6.2 Velocity and flow measurements

Experimental velocity measurements were performed in accessible locations in the flocculation unit. Velocity measurements were also carried out to estimate the flow division between the new and old flocculation sections in the plant. Measurements of the water velocity were also performed at the outlet of flocculation unit number 6. The description of the instruments used for measurements and how and where the measurements were made will be presented in the following sections.

6.2.1 Acoustic Doppler Velocimeter

To obtain velocity data inside the flocculation unit an Acoustic Doppler Velocimeter (ADV) was used. The ADV is designed to measure instantaneous velocities in three directions. The ADV probe head consists of one acoustic transmitter and three receivers. The acoustic transmitter sends out acoustic pulses which are scattered back to the three receivers by particles present in the water. The measuring point by the ADV is 5 cm below the transmitter (Lund & Jönsson 2002). The digital signal processing is done with a computer that has the ADV software installed.

6.2.2 Propeller type current meter

A propeller type current meter consists of a small propeller mounted on a metallic rod. The propeller is directed against the flow direction and rotates when water passes by. The number of propeller revolutions is registered by a meter connected to the propeller. The propeller revolutions can be converted to velocities by an equation associated to the specific propeller supplied by the manufacturer. The time length of the measurements should be noted for each measurement. This instrument should preferably be used when the flow direction is defined in one direction (Joseph 2014).

6.2.3 Velocity measurements in the flocculation unit

The flocculation tanks in the treatment plant are sealed and the access to the flocculation units is limited. Smaller windows of the flocculation units were, however, unsealed on the top where measurements could be taken. A smaller window with dimensions 0.8 x 0.5 m located on the top right corner of the flocculation unit number 1 could be accessed for measurements see Figure 6. The velocity measurements were carried out for the flocculation unit number 1 using an ADV instrument. The ADV was mounted on two horizontally metallic poles for vertical support and was fixated over the smaller window accessible for measurements. These two poles were fixated between the red handles see Figure 7. It was however difficult to keep the ADV vertically down in the flocculation unit so it was, additionally straightened and held with hand.

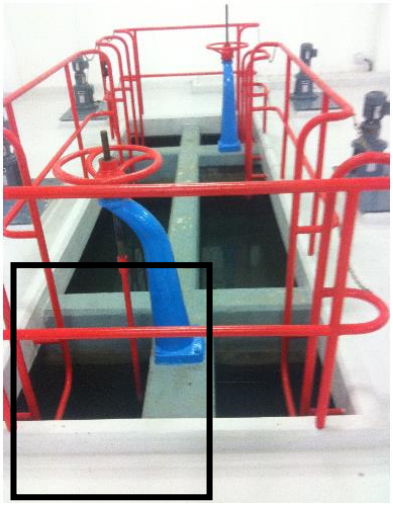

Figure 6. The window of the flocculation unit number one accessible for measurements (framed).

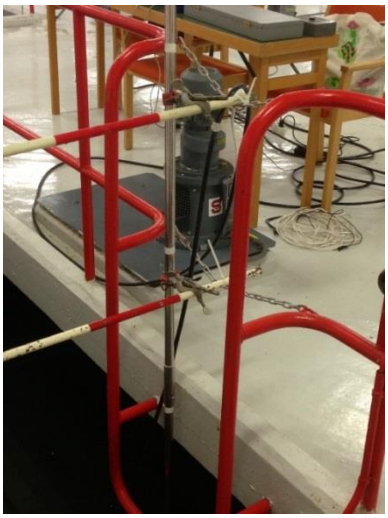

Figure 7. The ADV mounted on two horizontal poles fixated between the red handles.

Two surface points was chosen as measuring points, the surface points chosen can be viewed in Figure 8. Each point was measured at seven depths in the flocculation unit see Table 1.

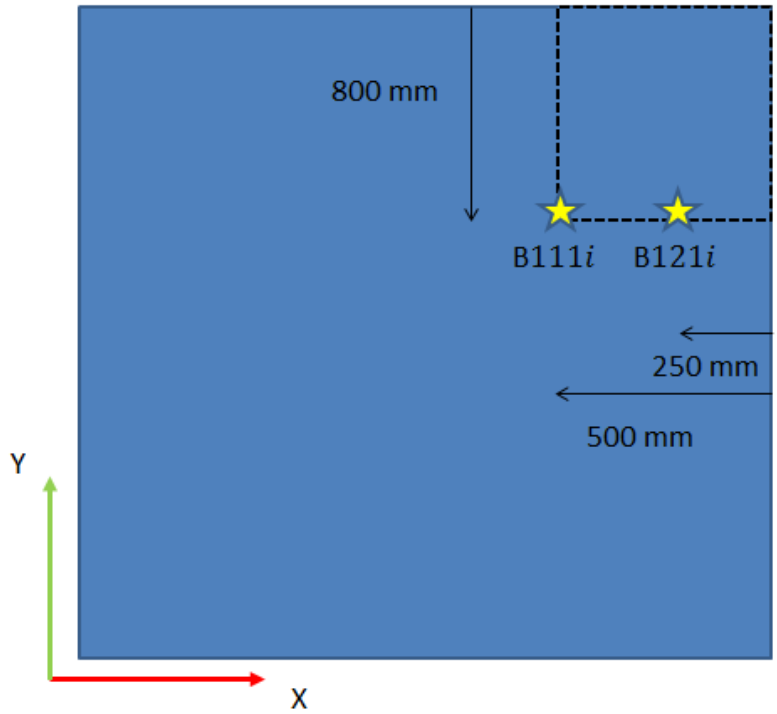

Figure 8. Schematic overview of the surface point's location used for measurements, where *i*= (1,2,3,4,5,6,7).

Table1. Table of points where velocity measurements were carried out.

Depths (mm)	Measurement points	
50	B1111	B1211
550	B1112	B1212
1050	B1113	B1213
1550	B1114	B1214
2050	B1115	B1215
2550	B1116	B1216
3050	B1117	B1217

6.2.4 Velocity measurements for flow division calculations

The velocity measurements for assessing the flow division Q2 and Q3 between the old and new flocculation sections have been done in measurement location 1 and 2 see Figure 9. The sectional areas of measurement location 1 and 2 have been measured in-situ using a standard ruler. The sectional areas can be seen in Figure 10.

The sectional areas of measurement location 1 and 2 have been sub-divided in 6 equal areas A_i, where *i*= 1, 2, 3, 4, 5, 6. In the middle of each of these areas velocity measurements have been carried out, V_i. To assess the flow in measurement location 1 and 2 equation (1) has been used:

$$Q_{Tot} = sum(A_i \times V_i) \qquad (1)$$

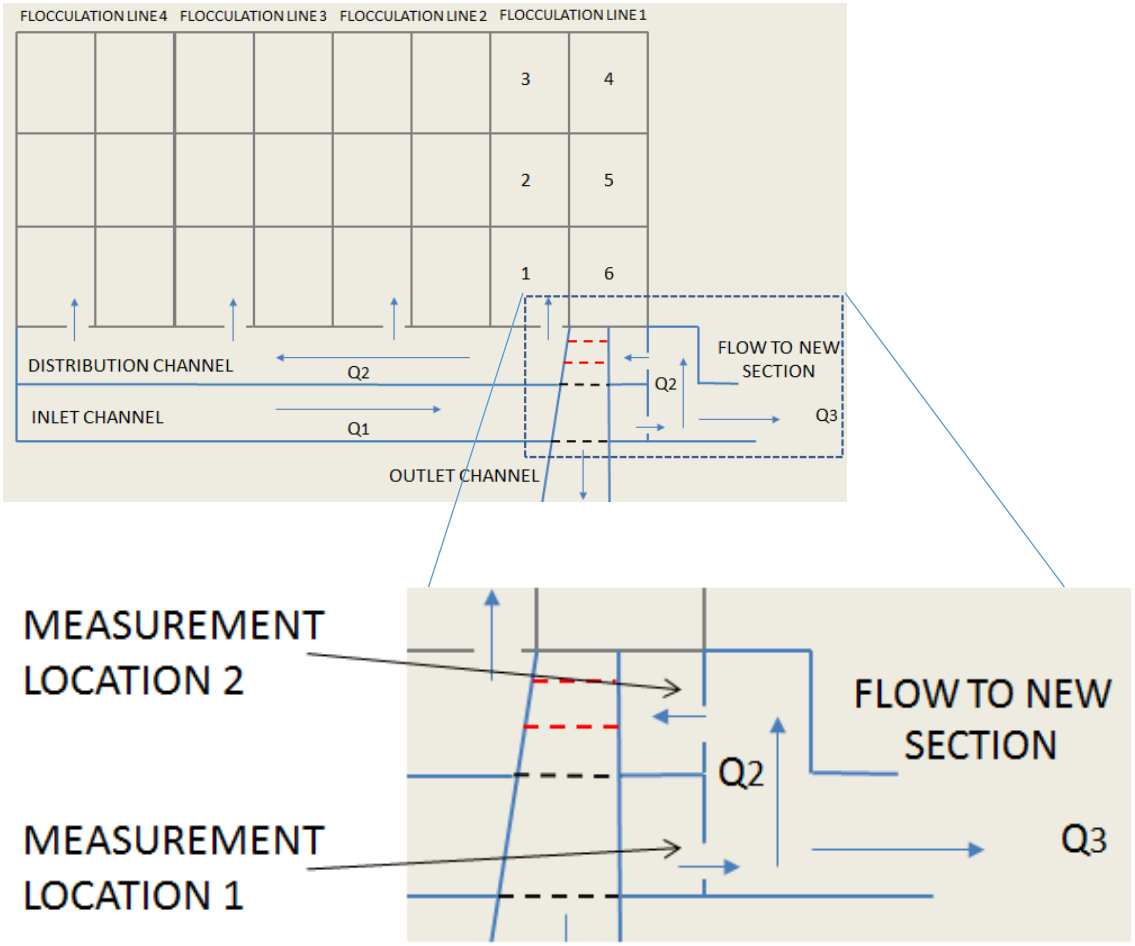

Figure 9. Close up on the two measurement locations where velocity measurements were carried out to estimate the flow division.

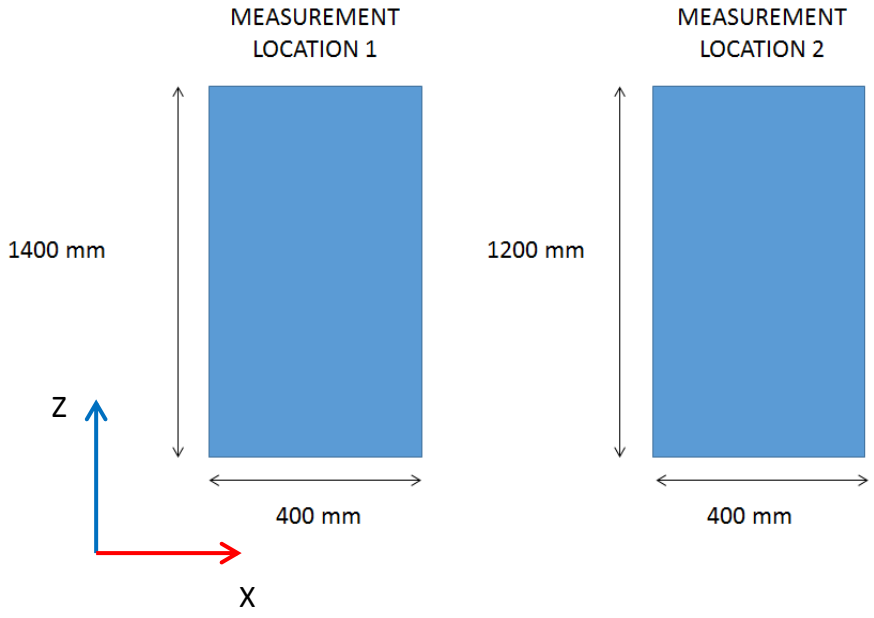

Figure 10. Sectional areas of the two measurement locations used for estimating the flow division.

The velocity measurements were carried out with a propeller-type current meter. It is reasoned that the flow direction can be defined in one direction. When the measurements were carried out the propeller-type current meter was held into position solely by hand in all measurements.

6.2.5 Velocity measurements at the outlet of flocculation number 6

Velocity measurements at several points at the outlet of flocculation number 6 were also carried out to have an estimate on how much water that enters the flocculation unit number 1. The velocity measurements were done using the ADV. The points in which the measurements were done can be seen in Figure 11. The ADV was put into positions and the outlet wall acted as vertical support.

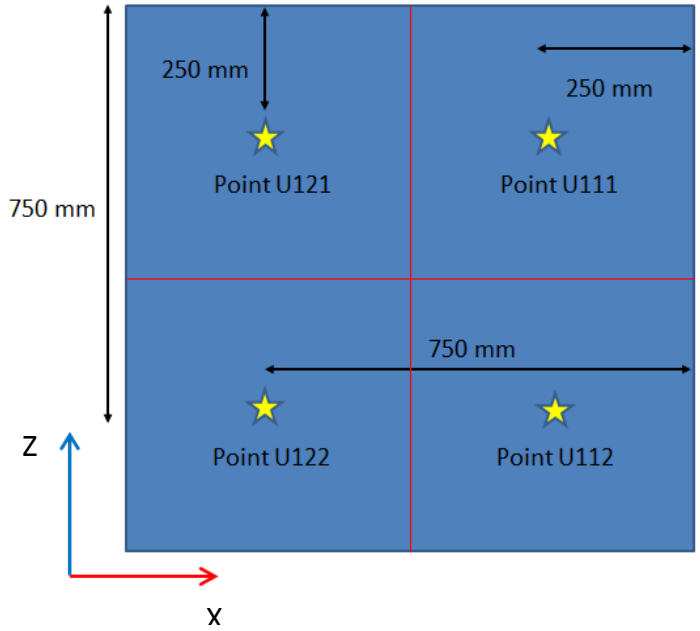

Figure 11. Section view of the outlet of flocculation number 6 and the locations for measurements.

6.3 Numerical model

To model the flow in the flocculation unit the following steps have to be carried out; constructing the geometry, setting up the computational mesh, and solving.

6.3.1 Geometry and mesh of the flocculation unit

The geometry of the flocculation unit has been described previously in Section 6.1 and Figure 5. *ANSYS Designmodeler* was used to generate a three-dimensional model of the flocculation unit. The computational geometry consists of a square shaped tank with a cylindrical region around the impeller. An inlet and an outlet exist also on the faces of the flocculation geometry. The two different geometrical shapes that exist in the geometry together with the inlet and outlet faces make the desired mesh outcome rather difficult to obtain. To meet this problem the geometry was sub-divided into fourteen parts prior subsequent step of meshing to permit "*Sweep meshing*". The geometry was modeled as two parts, one part being the tank multi-body part (stator) and the other being the inner rotational impeller region (rotor).

Meshes can be categorized in structured and unstructured meshes. The structured meshes are called hexahedral elements in 3D. Unstructured meshes are as the name implies

composed of unordered cells and, consist of hexahedral, tetrahedral, prisms, and pyramid elements in 3D (Hirsch 2007). Hexahedral elements give better accuracy and fewer cells can be used when meshing the same geometry (Andersson 2011). For these reasons the flocculation unit was "Swept" with hexahedral elements in all parts of the tank except the rotor where tetrahedral elements were used.

In the near wall regions the viscous forces are more dominant than the inertial forces this makes turbulence models inapplicable here (Andersson 2011). For this reason inflation layers have been constructed in these areas. Inflation layers have been constructed for tank walls, tank bottom, and impeller. In these areas wall functions have been used.

For the mesh generation *ANSYS meshing* was used. Due to the flocculation geometry's complexity the function *Worksheet recording* in *ANSYS meshing* was used to define the order of meshing of the different tank parts to obtain desired mesh outcome. Adaptation of the mesh was performed with regards to velocity gradients in the rotational region and the tank part just outside. The number of cells used in presented simulation are 1 941 197 cells with an aspectration of 21.8 (mostly inflation) and skewness 0.95.

6.3.2 Solving

ANSYS Fluent has been used to model the hydrodynamics in the flocculation unit. To reduce round-of errors in calculation the double precision solver was used (ANSYS 2013). The coupled solver scheme was used and the simulations were performed with second-order upwind spatial discretization scheme. To model the flocculation hydrodynamics the Sliding mesh (SM) modelling approach was used in combination with the renormalized group k-ε (RNG k-ε) turbulence model. Since the ratio between the impeller diameter and the width of the flocculation unit is relatively high (0.61) a transient behavior at the interface between rotor and stator is likely to be seen therefore the SM modelling approach was chosen (ANSYS 2013). The following boundary conditions have been used; the inlet was specified as a velocity inlet, the outlet of the tank was specified as a pressure outlet. The water surface was not modelled instead it was treated as a wall. The turbulence intensity at the inlet was calculated by calculating the Reynolds number (Re) at the inlet. The equation for estimating turbulent intensity is as follows (Andersson 2011):

$$I = 0.16 \times Re^{-1/8} \qquad (2)$$

The boundary conditions are given in Table 2. Surface monitoring on volume flow rate at the outlet was done to evaluate convergence. The limit on scaled residuals for estimating convergence for continuity, x-velocity, y-velocity, z-velocity, turbulent kinetic energy (k), and turbulent energy dissipation (ε) was set to $1x10^{-4}$.

Table 2. Boundary conditions for the numerical model.

BOUNDARY CONDITIONS	
Inlet velocity (m/s)	0.029
Impeller velocity (m/s)	0.41
Turbulence intensity inlet (%)	4.48
Turbulence intensity outlet (%)	5.0

7. Results and discussion

The results from the experimental measurements and the numerical modelling in addition with discussion and analysis of the results will be presented here. The coordinate system in which the measurements were taken and the numerical model was constructed can be seen in Figure 12.

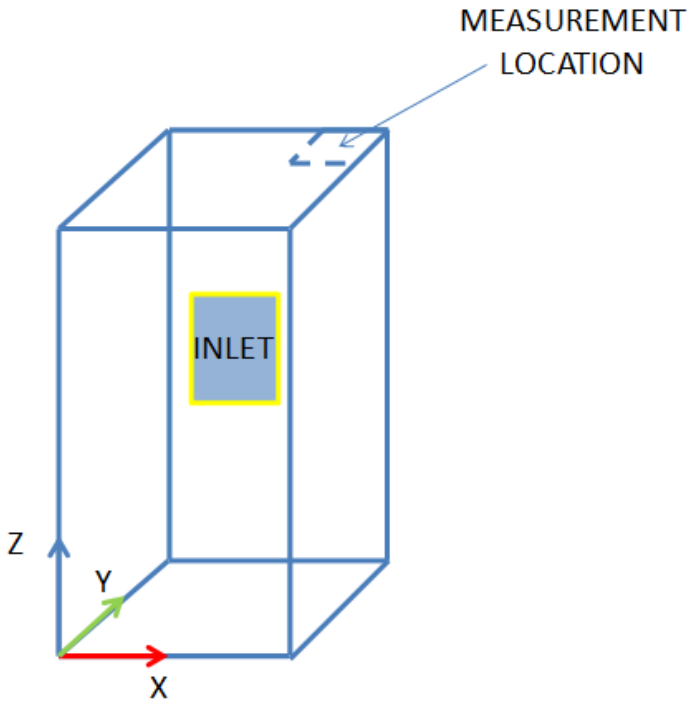

Figure 12. Coordinate system definition for measurement taking and geometry construction. Origo is located at the bottom left corner of the unit on the inlet side Cartesian coordinate system.

7.1 Experimental results

In this section the experimental results from the study will be presented.

7.1.1 Experimental measurements on velocity in the flocculation unit

The measurements were performed in the upper right corner of the flocculation unit, Figure 13. The rotation in the flocculation unit is clockwise and the rotational velocity is v= 0.41 m/s a value supplied by the plant. The expected flow direction in the unit can also be seen Figure 13. At the day of the measurement the water temperature was T = 9.92°C.

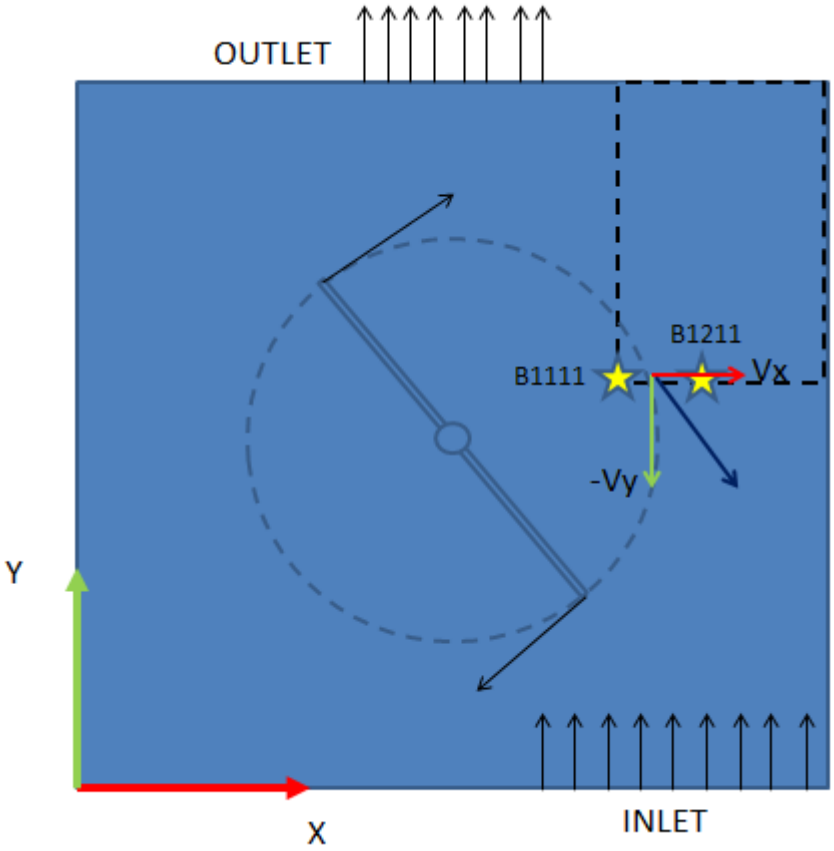

Figure 13. Schematic overview of the location for the measurement points and the expected flow direction in the unit.

Each velocity measurement was carried out for approximately 60 s. Generally, when measuring the velocity using the ADV probe, the velocity measurements demonstrates a fluctuating velocity profile, Figure 14 and 15. The variations in the velocity are mainly caused by the rotational movements of the propeller. These variations are more dominant closer to the propeller, Figure 15.

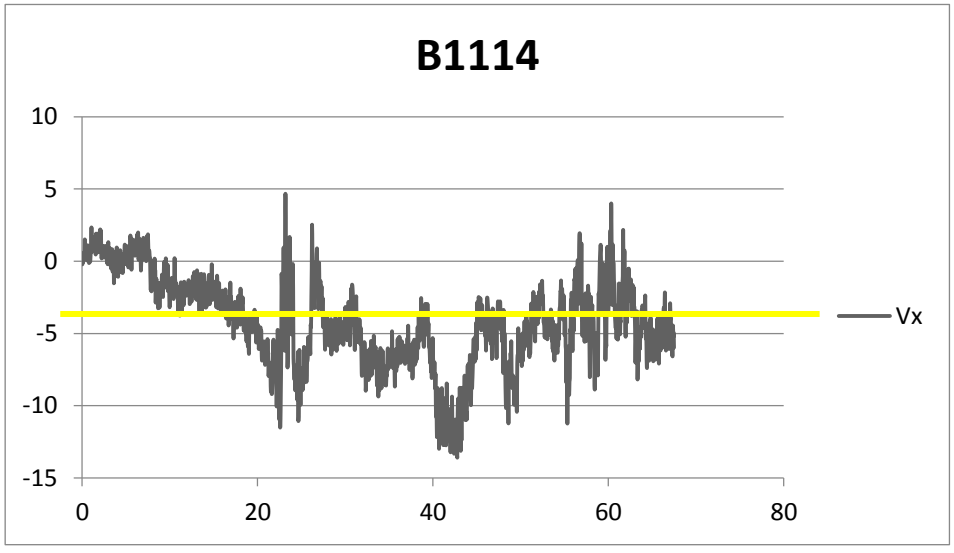

Figure 14. Velocity fluctuations for measurement point B1114.Yellow line represent the mean velocity.

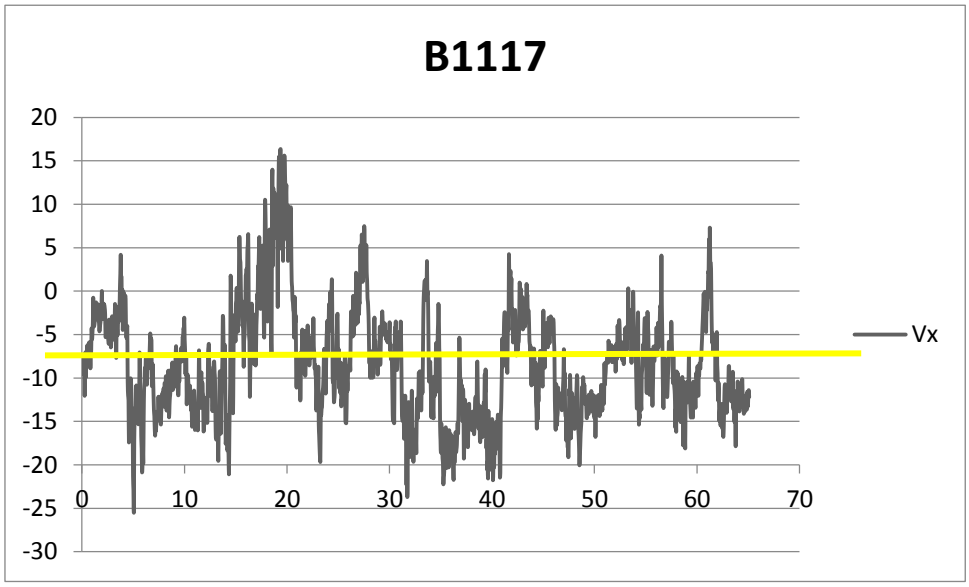

Figure 15. Velocity fluctuations for measurement point B1117.Yellow line represent the mean velocity.

7.1.2 Measurement line B111i

The y-velocity component in points B1111-B1117 was predominantly in the negative y-direction and this with a high frequency see Table 3. The measuring point B1114's mean y-velocity however deviates from the other measurement points and shows a smaller velocity magnitude in the negative y-direction. The measuring point B1114's depth coincides with the depth of the inlet bulk flow and this could have affected the velocity magnitude in this point.

Furthermore, the mean x-velocity components are predominantly in the positive x-direction see Table 3. The relative lower frequency of x-velocities in the positive direction could arise from disturbances of the flow due to the tank wall. The tank wall can lead to that the flow is "bounced" back and redirected in the negative x-direction near to the measuring points. It is also worth noting that the measuring point B1114 shows a negative mean velocity and a relatively low frequency of positive x-velocities. The inlet can have had an effect on this measuring point considering the inlets location. The flow pattern created by the impeller is not so easy to estimate beforehand and the negative mean x-velocities in point B1114 can be related to the created flow pattern as well.

Mean z-velocities for points B1111-B1117 are mainly positive see Table 3. The impeller in the flocculation unit is designed to pump down and later allow the flow to redirect and flow upwards in the positive z-direction. This could have had an effect on the velocities especially for the measuring points closer to the impeller.

7.1.3 Measurement line B121i

The measurements B1211-B1217 with regards to y-velocity direction seems to be similar to the measurements taken for measurement line B111i. The velocity direction is predominantly in the negative y-direction and the negative y-velocity frequency is still high, Table 3. The mean velocity magnitude is, however, slightly lower for points B1211-B1217 than for the measurements taken for measurement line B111i for points located on the same depths.

When it comes to measured x-velocity components for measurement line 2 the results are similar to the measurements along line B111i, Table 3. The x-velocity direction is mainly in the positive direction. The mean velocity magnitude is however little lower than for the measurements done in measurement line B111i. This can also be explained by the fact that these measurements are taken further away from the rotational center. It is likely that the direction of the velocity is influenced by the wall of the tank. Measurement point B1214 which corresponds to point B1114 in previous measurement line shows similar deviation in mean x-velocity and low frequencies of positive x-velocity frequency.

High positive mean z-velocity values can be seen for almost all measurement points in line B121i see Table 3. What is interesting to see is the relatively low negative z-velocity frequency in points B1215-B1217. Here one can assume that the flow is predominantly in the upward direction and is affected by the upcoming water generated by the impeller rotation.

7.2 Estimated flow pattern in the flocculation unit from measured velocity data

The flow pattern in the flocculation unit can be viewed using the measured velocity data. Almost all velocities in both measurement lines show a positive mean x-velocity component. However, points B1114 and B1214 show negative mean x-velocity components with high frequencies in the negative x-direction. The mean z-velocity components are also positive in most of the measurement points. Based on these observations, a sectional view of flow pattern for the points B1111-B1117 and B1211-B1217 has been made, Figure 16.

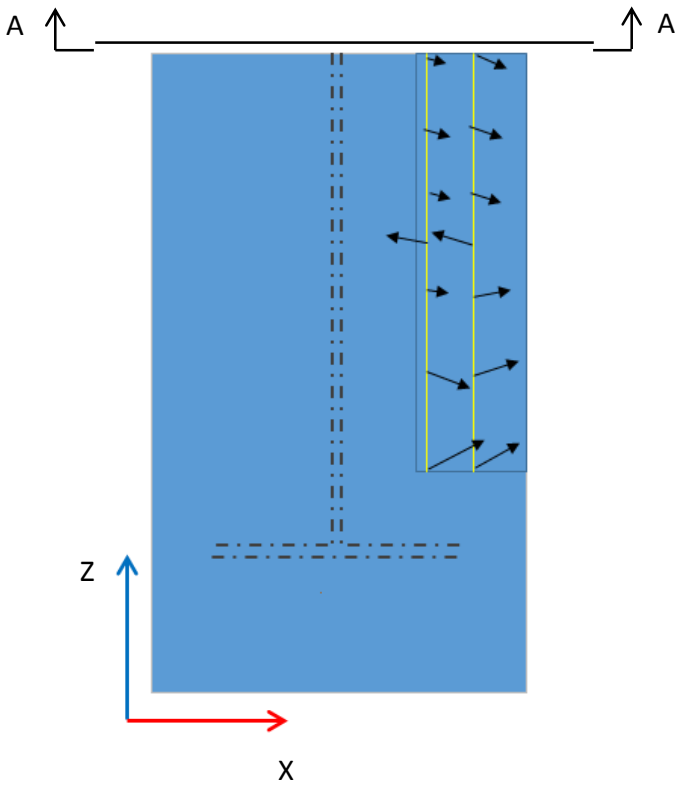

Figure 16. Estimated flow pattern in flocculation unit for measurement points B1111-B1117 and B1211-B1217.

Table 3. Measurement point locations in 3.05 m's depth from the water surface, mean velocity components Vx, Vy, Vz for measurement points, and percentage of positive Vx, negative Vy, and negative Vz for each measurement point.

LOCATION	X (mm)	Y (mm)	Z (mm)	MEAN Vx (cm/s)	% OF POSITIVE Vx	MEAN Vy (cm/s)	% OF NEGATIVE Vy	MEAN Vz (cm/s)	% OF NEGATIVE Vz
MEASUREMENT LINE 1									
B1111	1950	1650	5060	1.62	80	-7.73	99	0.08	43
B1112			4560	-0.61	42	-5.05	99	-0.85	65
B1113			4060	1.24	56	-5.56	95	0.38	50
B1114			3560	-1.62	35	-4.23	88	0.07	35
B1115			3060	1.23	62	-7.77	97	-1.21	60
B1116			2560	2.11	63	-7.93	95	1.10	50
B1117			2060	5.21	75	-7.47	90	0.28	55
MEASUREMENT LINE 2									
B1211	2200		5060	0.61	61	-5.39	98	-0.51	65
B1212			4560	0.37	56	-5.82	98	2.45	20
B1213			4060	0.52	57	-4.35	93	0.003	48
B1214			3560	-4.59	10	-5.77	93	2.84	33
B1215			3060	-0.46	49	-7.86	98	1.77	35
B1216			2560	0.22	49	-8.74	93	3.35	37
B1217			2060	0.37	51	-8.86	95	2.83	37

The initially expected flow direction can be seen in the flow pattern in Figure 16. There are sources of errors that should be considered. Each velocity measurement was made individually. To obtain a better estimation of the flow pattern in the flocculation unit several Acoustic Doppler Velocimeters (ADV's) could have been used for measurements simultaneously. The obtained flow pattern from the measurements is realistic but it's hard to draw definite conclusion whether it's realistic or not. If the water was just swirling around in the unit in circular motion as the impeller rotates then it would have been easier to draw definite conclusions from the results. However this is not the case the water mainly flows in the vertical direction in the unit and probably gives rise to complex flow pattern. In previous research made by Peltier et al. (2013) it was shown that even a slight misalignment of the ADV in the horizontal plane can give rise to large errors in x-velocity components. Furthermore, it is mentioned by Peltier et al. (2013) that the error in y-velocity components rarely exceeds 5 % even with a small misalignment. A mismatch between the ADV's coordinate frame and the reference frame in the tank could have had an effect on the relatively lower positive y-velocity frequencies that could be seen above. Furthermore, the usage of an acoustical instrument like the ADV can cause velocity spikes into the velocity data due to noise disturbances (Chanson et al. 2008). Such noise disturbances can be the doppler noise or noise generated from the vicinity of the ADV. Velocity spikes can have affected the calculated mean values above. Post-processing of the measurement data could be made with regards to velocity spikes prior evaluating the measurements. Such post-processing of ADV velocity spikes can be the use of various filtering and replacement methods like the phase-space filtering method and the Last Good Value (LGV) replacement method. The filtering methods filters out the velocity spikes and the replacement methods replace the velocity spikes with a more suitable value (Jesson et al. 2012).

7.3 Experimental measurements on flow division

The flow division location can be viewed in Figure 17 and data for the flow division calculation can be viewed in Table 4-5.

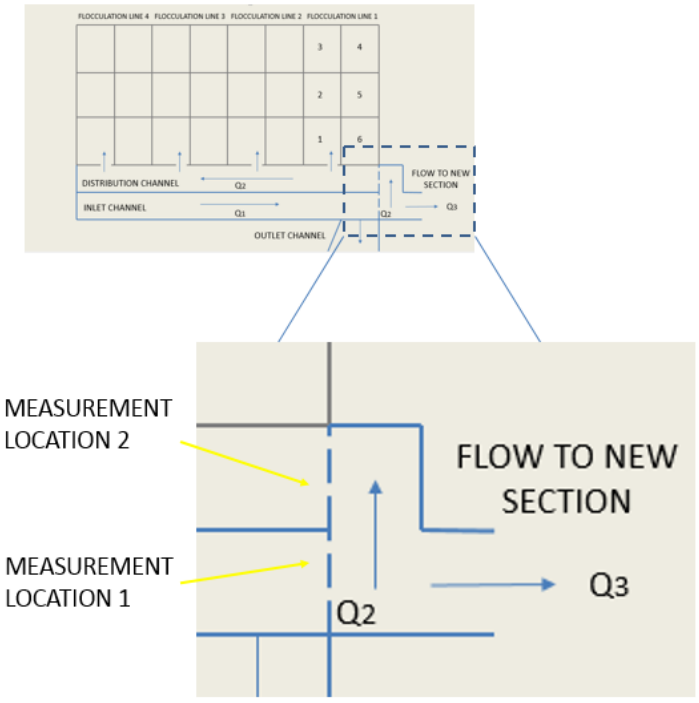

Figure 17. Measurement locations for the flow division calculation.

Table 4. Indata for flow division assessment: measurement location 1.

MEASUREMENT LOCATION 1			
POINT	MEAN PROPELLER REVOLUTIONS/S	VELOCITY SUB-DIVIDED AREA (m/s)	SUB-DIVIDED AREA (m2)
1	2.83	0.205	0.096
2	3.25	0.227	0.096
3	1.96	0.159	0.096
4	2.88	0.208	0.096
5	2.46	0.180	0.096
6	3.51	0.241	0.096

Table 5. Indata for flow division assessment: measurement location 2.

MEASUREMENT LOCATION 2			
POINT	MEAN PROPELLER REVOLUTIONS/S	VELOCITY SUB-DIVIDED AREA (m/s)	SUB-DIVIDED AREA (m2)
1	0.60	0.086	0.08
2	2.0	0.161	0.08
3	4.3	0.306	0.08
4	1.0	0.108	0.08
5	4.23	0.279	0.08
6	3.16	0.223	0.08

The equation for converting mean revolutions/s to m/s is supplied by the propeller current meter manufacturer where the velocity (V) is calculated as

$$V = 0.055 + n \times 0.0531 \qquad (3)$$

where *n* is the mean propeller revolutions/s.

In measurement location 1 a flow Q1 of 117 l/s was calculated using equation 1. In measurement location 2 a flow Q2 of 93 l/s was calculated. This says that a flow of 93 l/s is entering the old flocculation section and a flow Q3 of 24 l/s is flowing to the new flocculation section, Figure 9. The flow Q1 (in measurement location 1) was according to the water treatment plant 200 l/s. The flow Q2, after flow division, was thought to be 70 % of Q1. The remainder 30 % was believed to enter the new section as Q3. There exist many possible reasons why the propeller current meter underestimated the velocity. One reason can be that the propeller can have been misplaced and not put normal to the subdivided areas or that the flow was not normal to the measurement locations. The measurements were carried out during 60 s. This could perhaps have been longer to get better statistics. The ADV instrument could have been used here as well to obtain more reliable velocity measurements.

7.4 Assessment on flow rate out of flocculation unit 6

In order to assess how much water that enters flocculation unit number 1 velocity measurements in several points on the outlet flocculation number 6 were made. The measurement time was approximately 120 s for every measurement. In similar way as to the calculations of flow division the outlet was subdivided in several equally large areas see Figure 18 for measurement points and subdivision.

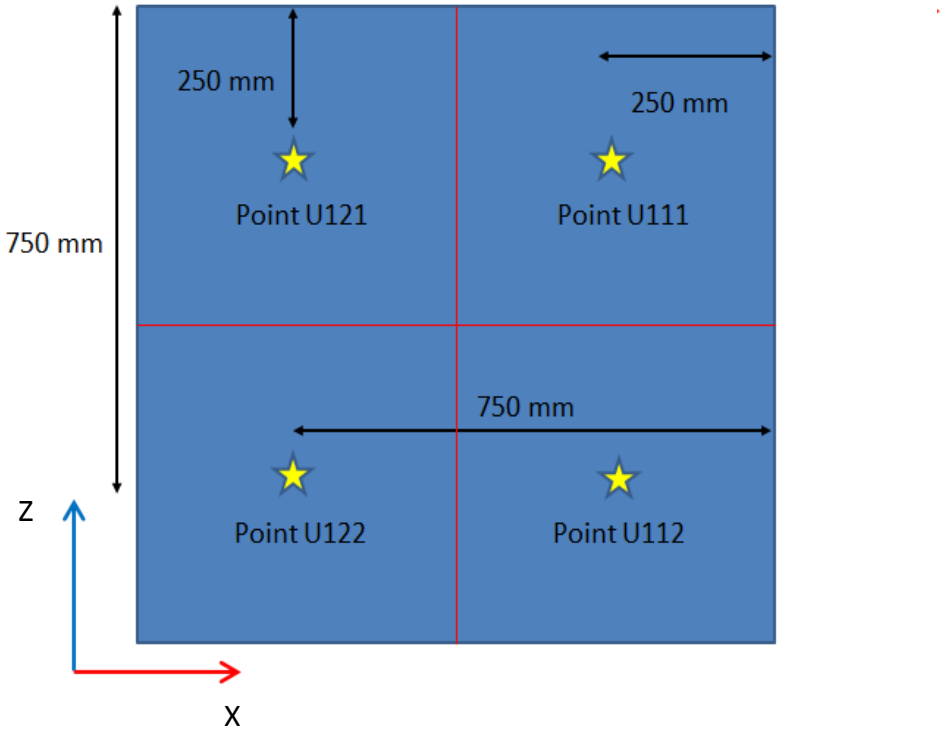

Figure 18. Measurement points and subdivisions of outlet of flocculation number 6.

The calculation for flow can be made by equation 1. The ADV gives velocities in three directions for every measurement point in on the outlet and every measurement were taken for approximately 120 s. The velocity of interest for flow calculation is the y-velocity component normal the subdivided areas. In Table 6 the y-velocity component and calculated flow for the measurement points can be seen.

Table 6. Mean Y-velocity and calculated outflow from the outlet.

POINT	MEAN Y-VELOCITY (m/s)	SUBDIVIDED AREA (m2)	OUTLET FLOW (m3/s)
U121	0.032	0.25	0.0080
U111	0.032	0.25	0.0080
U122	0.026	0.25	0.0065
U112	0.022	0.25	0.0055
			SUM : 0.028

The total outflow from flocculation number 6 resulted in 0.028 m^3/s which is equivalent to 28 l/s. If 28 l/s is assumed to enter each and every one of the four flocculation treatment lines the sum of all flow entering the old flocculation section as Q2 is equal to 112 l/s. This value lies close to the previously calculated value of 93 l/s for Q2 in previous section. If the flow division is assumed to be 70% and 30% respectively the flow Q1 would result in 160 l/s and flow Q3 in 48 l/s.

7.2 Numerical results

This section is divided into the sections geometry, mesh and solution results.

7.2.1 Geometry and mesh results

The geometry was made in *Ansys designmodeler*. Images on the constructed geometry from the viewpoints; front-view, isometric-view (iso) and top-view can be seen in Figure 19-21. For the mesh a side-view, a top-view and a view inside the impeller region can be seen in Figures 22-25.

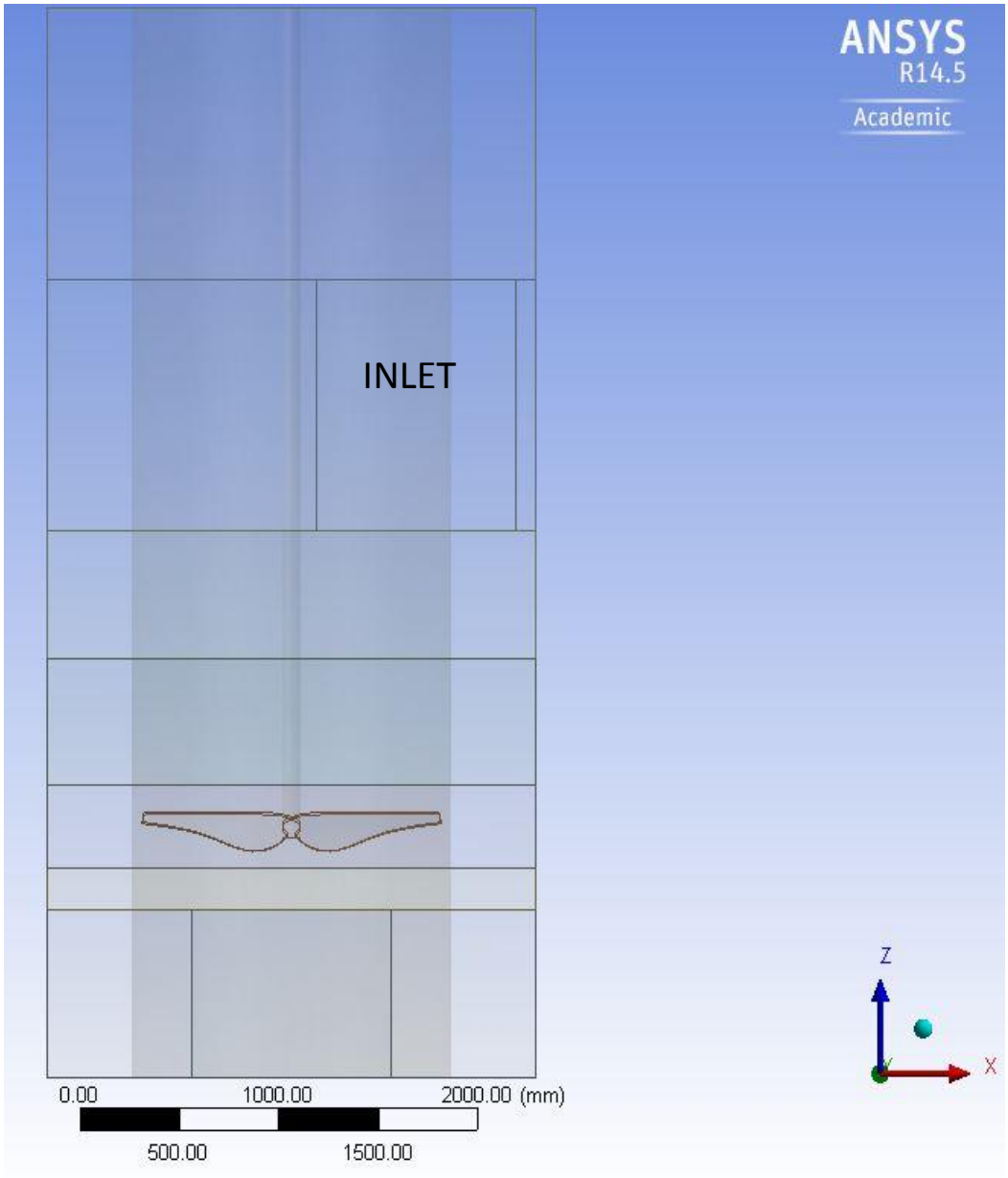

Figure 19. Front-view of flocculation unit number 1.

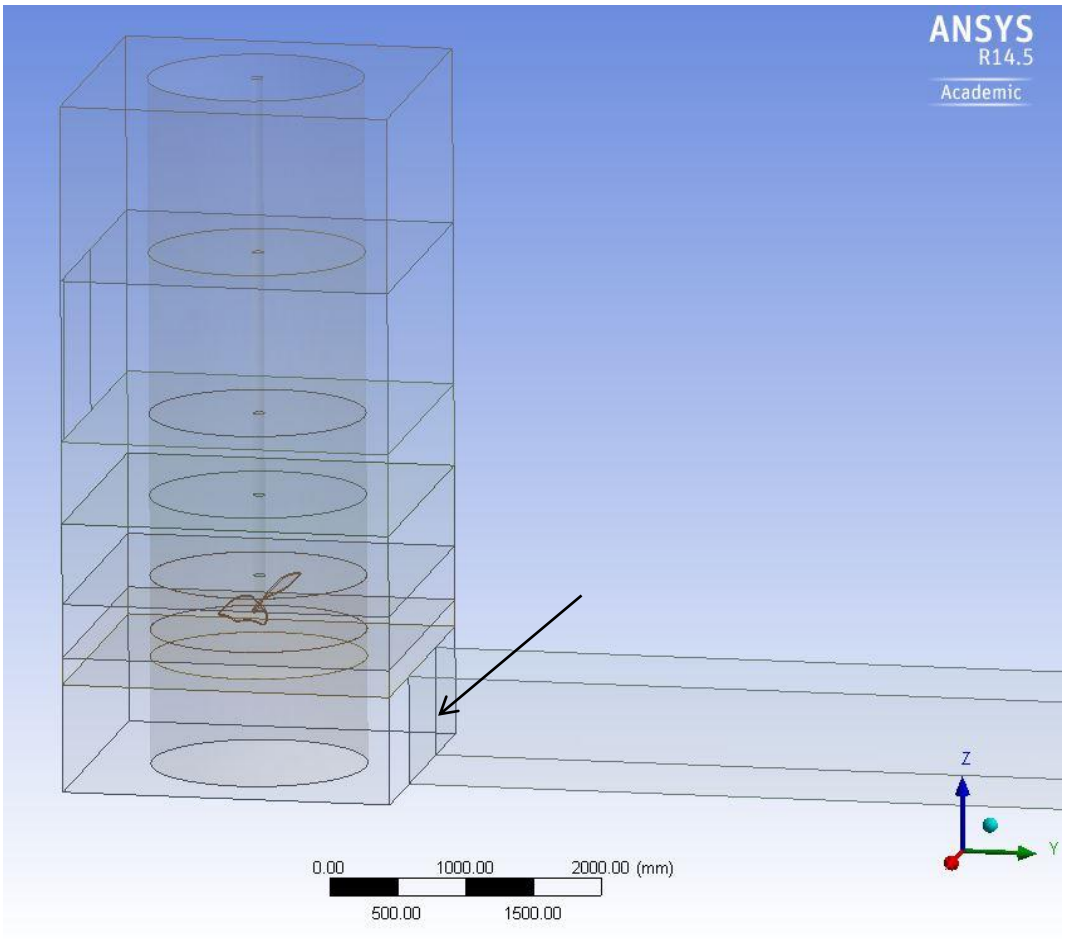

Figure 20. Iso-view of flocculation number 1.

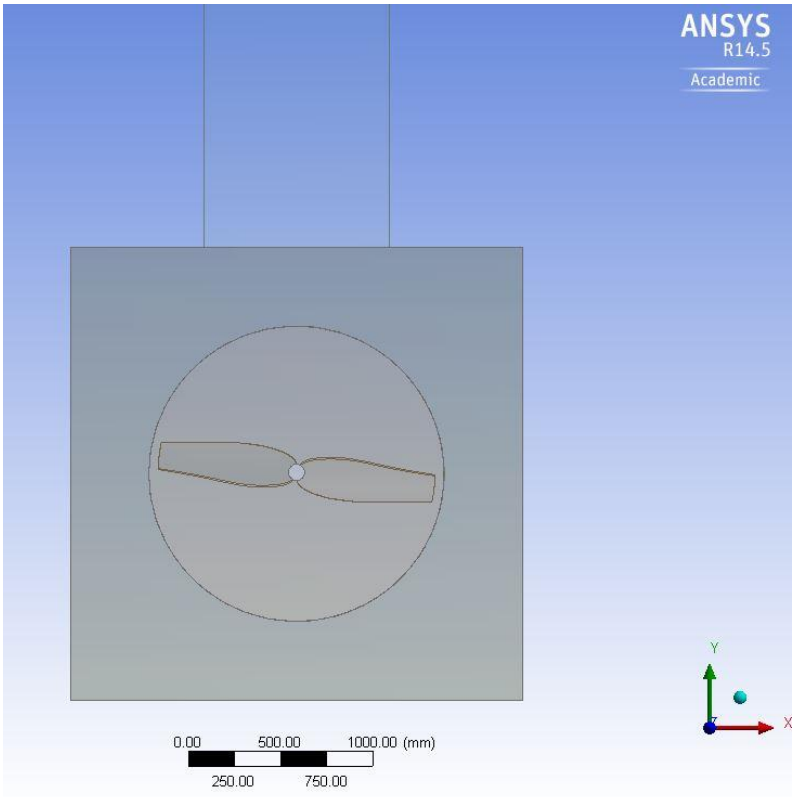

Figure 21. Top-view of flocculation unit number 1.

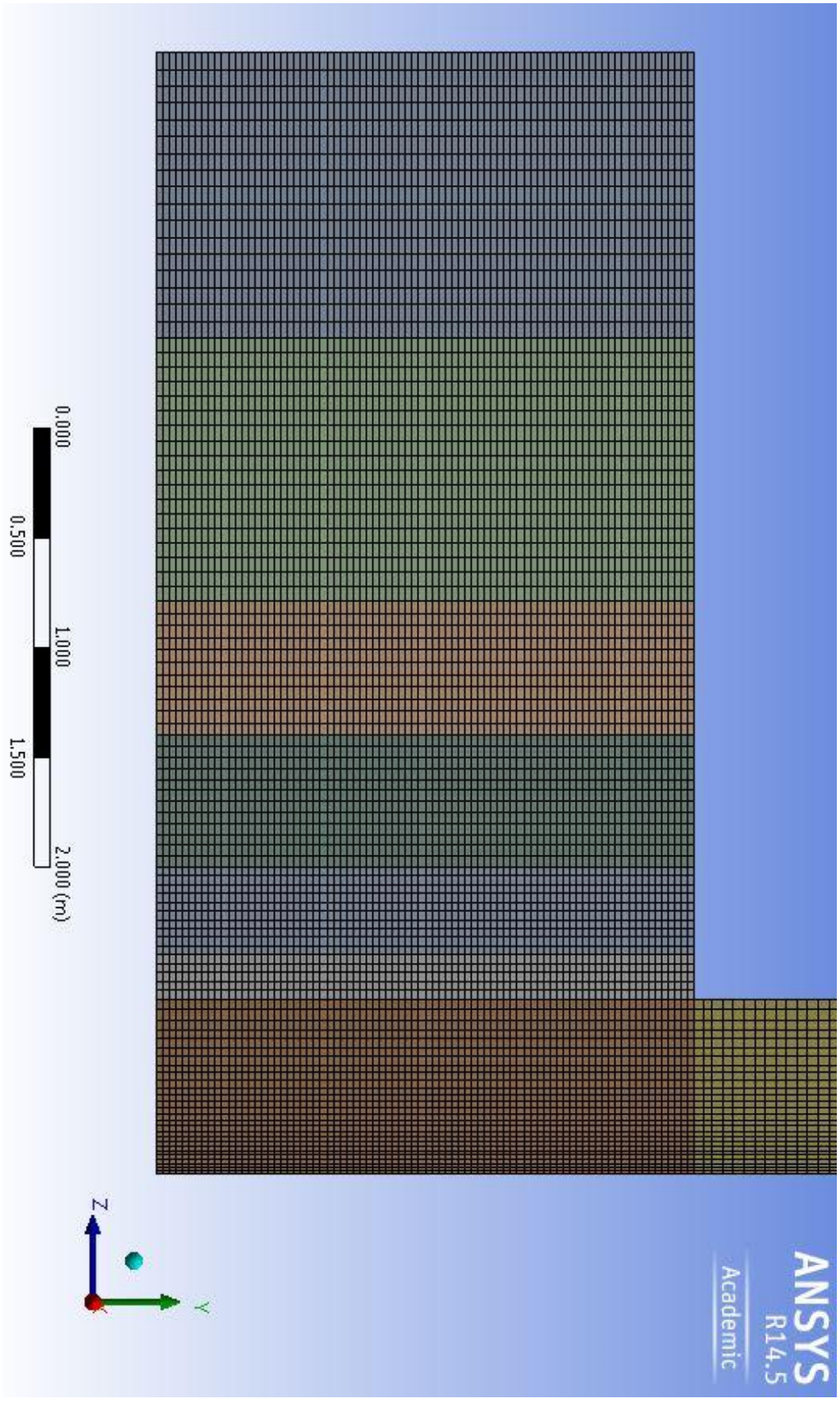

Figure 22. A Side-view of the computational mesh for flocculation tank number 1.

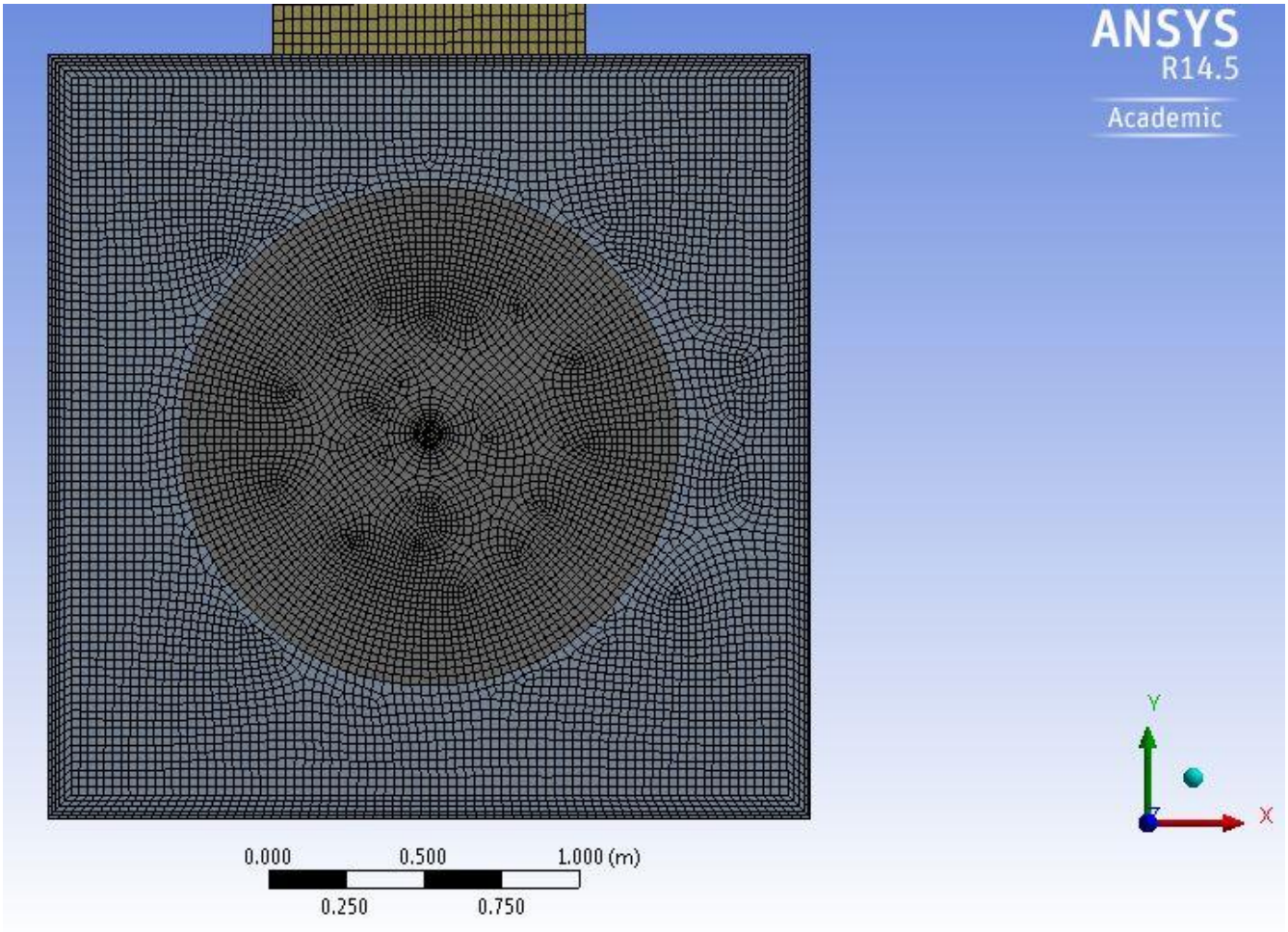

Figure 23. A top-view of the computational mesh for flocculation unit number 1.

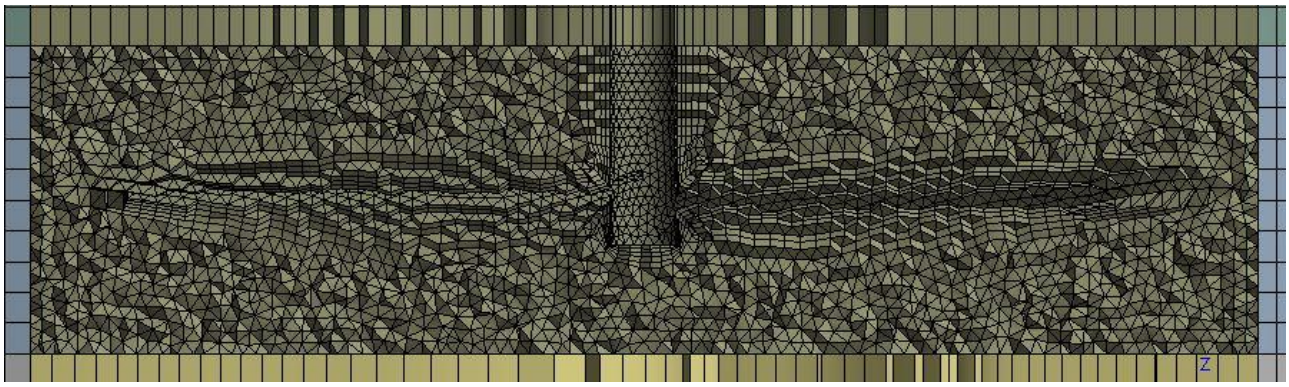

Figure 24. A view of the computational mesh inside the impeller region.

7.2.2 Solution results

The results from the numerical simulation will be presented in the form of vector plots, contour plots, and graphs. Both multiple reference frames (MRF) and sliding mesh (SM) modelling approach was tested but only the SM case converged. The case presented has been simulated for 250 s. Due to the difficulties of convergence and available computational power for the master thesis project, no successive mesh refinements could be carried out. Therefore a more refined mesh could bring about more accurate results. However, some general aspects of the outcome of this work will be presented and discussed in the following.

7.2.2.1 Convergence

The convergence criteria for the simulation were set to a scaled residual of 10^{-4}. For parameters x-velocity, y-velocity, z-velocity, k (turbulent kinetic energy), and ε (turbulent energy dissipation rate) the scaled residual fell well below the set limit except for the continuity equation which were approaching this limit see Figure 25.

```
Updating solution at time level N... done.
  iter  continuity  x-velocity  y-velocity  z-velocity           k     epsilon outlet-flow point-b1117     time/iter
 68167  3.9131e-05  1.1113e-08  2.1408e-08  1.9553e-08  5.4391e-08  6.8153e-08 -3.4800e-02 -3.7922e-02  0:13:18   30
```

Figure 25. Snapshot from the Fluent TUI (text user interface) that show the different scaled residuals for the parameters at iteration 68 167.

To asses convergence the volumetric flow rate at the outlet of the flocculation unit was monitored. The volumetric flow rate at the inlet should be equal to the volumetric flow rate at the outlet to have continuity in the system. An inlet velocity of 0.029 m/s and an inlet sectional area of 1.2 m give a volumetric flow rate at the inlet of 0.0348 m^3/s. The volumetric flow rate at the outlet was achieved to be equal to the volumetric flow rate at the inlet. Furthermore, considering the velocity of the water pumped down by the impeller which is approximately 0.1 m/s and the height of the tank which is 5.11 m the water would have travelled in the whole tank in approximately 100 s. The final simulation time was 250 s together with all other convergence criteria being met the solution can be considered converged.

The mass imbalance is described as the net of the mass entering each cell and mass leaving each cell. A general guideline is that the mass imbalance is less than 1% of the smallest flux through the system (Ansys 2013). The flux through the system is 34.8 kg/s (derived from the volumetric flow rate in the system). As can be seen from Figure 26 the maximum mass imbalance is $3.0e^{-3}$ and the minimum is $-4.63e^{-5}$ in the system. A local maximum mass imbalance can be seen in the interface between rotational region and stationary region. Nevertheless the mass imbalances in the unit are much less than the guideline value and the conservation of mass can be said to be fulfilled.

Figure 26. Contours of mass imbalance for Y=1225 mm.

7.2.2.2 Hydrodynamics in the flocculation unit

The hydrodynamics in the flocculation unit can best be viewed in vector plots that show both velocity direction and velocity magnitude. The velocity plots have been taken in strategic locations to understand the flow pattern in the unit. The sections where vector plots were taken are Z= 3600 mm, Z= 2000 mm, Z= 1200 mm, Y= 1225 mm and diagonal section through the flocculation unit see Figure 26. The impeller is located in the center of the flocculation unit looked from the top view of Figure 27.

In a section Z= 1200 mm it can be seen that the impeller sucks the water in the unit to the centre to later pump it down, Figure 28. Swirls like the ones that can be seen in section Z= 2000 mm are not created in this section probably due to the proximity to the rotational region and the higher water velocities that can be seen here. What is worth noticing is that if one look at a planar view of section Z=2000 mm one can see that local swirls are formed closer to the tank corners and the tank centre see Figure 29. The tank corners in this case acts like baffles and induces swirl motion which increase mixing. These areas together with the circulation loops formed around the impeller that can be seen in Figure 31 and 32 are probably areas of high floc growth rate due to higher rates of mixing. Too high shear can however lead to flock breakage.

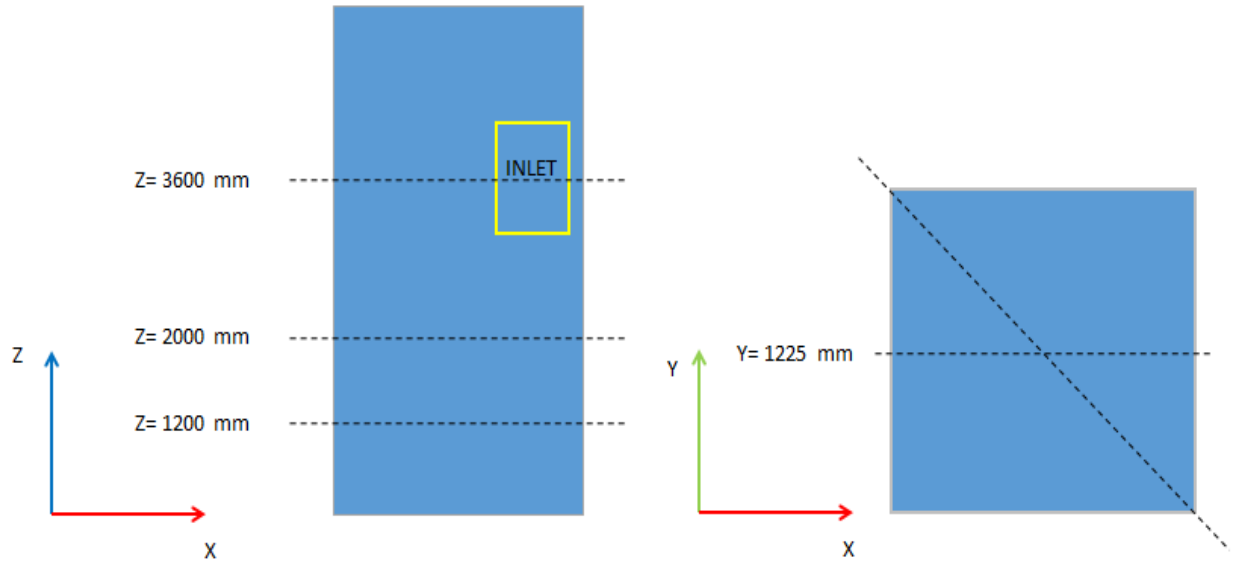

Figure 27. Sections where presentation of vector plots and contour plots will be made. Left: front view of unit. Right: top-view of unit.

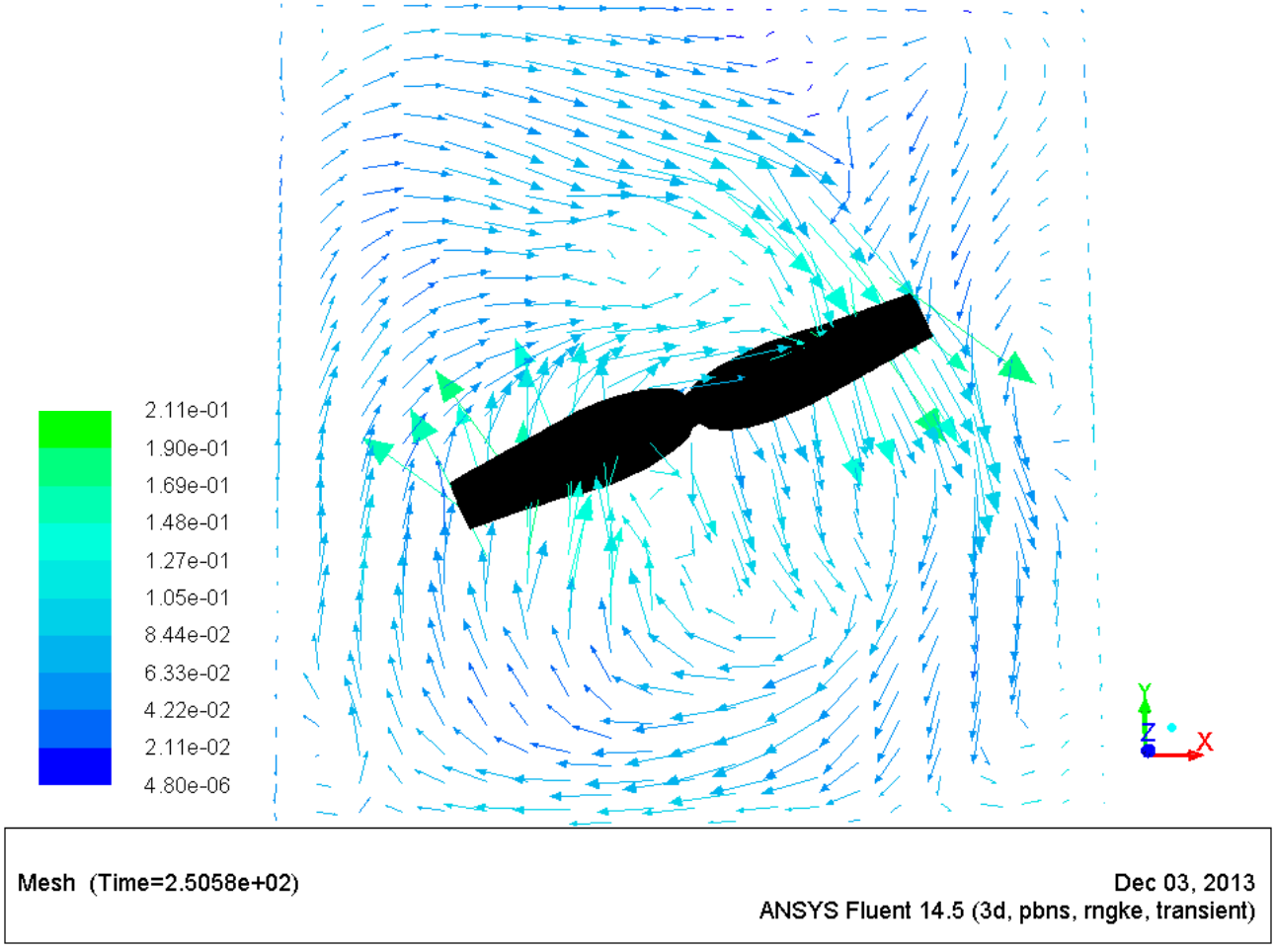

Figure 28. A top view of section Z=1200 mm in the unit. The impeller is located in this section.

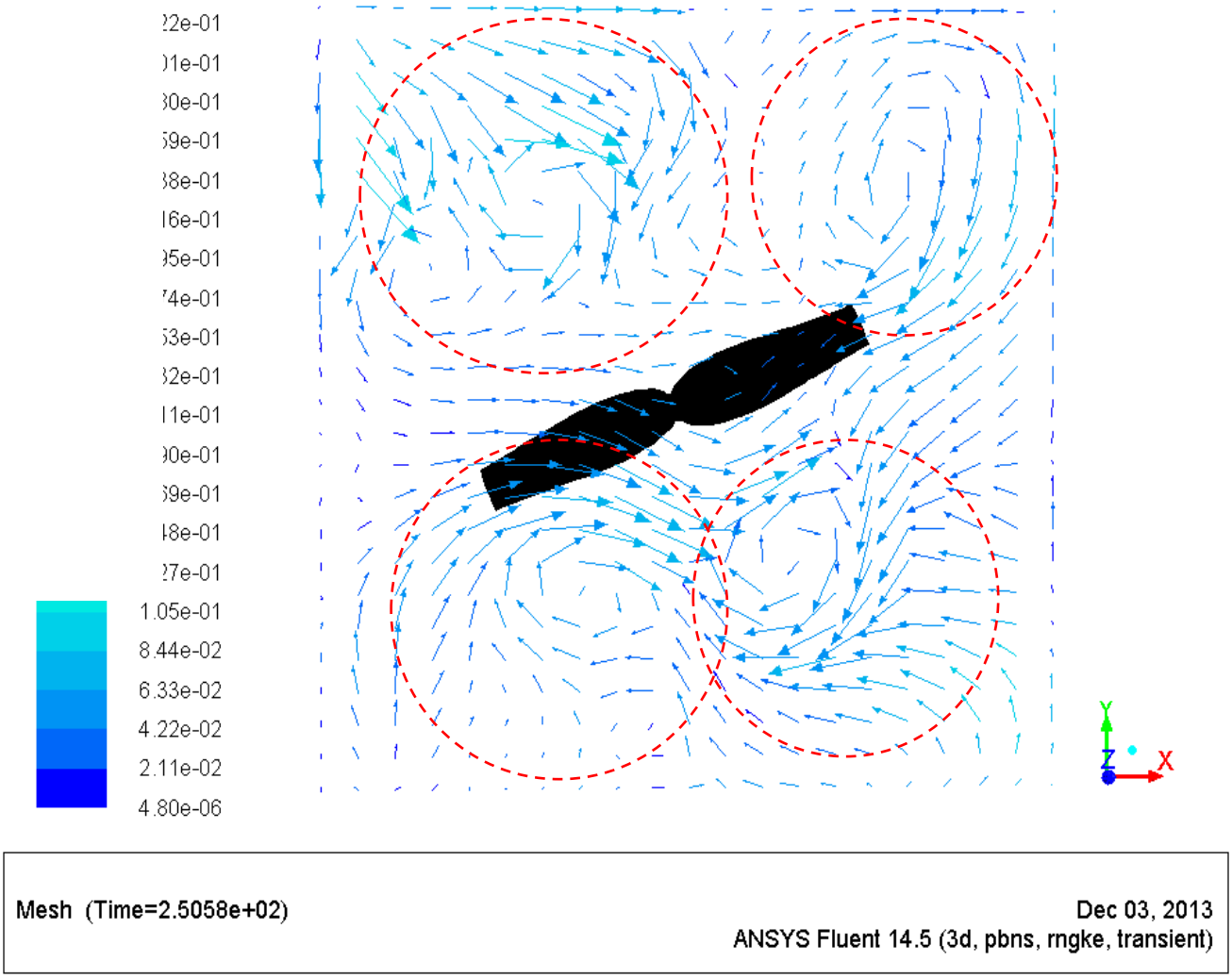

Figure 29. A top view of section Z= 2000 mm. Swirl motions formed due to tank corners. Impeller is located below this section.

In the experimental velocity measurements it could be seen that measurement points B1114 and B1214 had a deviating mean x-velocity and x-velocity direction. The reasons for this deviating mean y-velocity was initially described as being the effects of the inlet. The inlet has some effect on these points but also the flow pattern generated by the impeller has perhaps a greater effect on the measurement location. In section Z= 3600 mm which roughly corresponds to the Z-distance of points B1114 and B1214 the numerical model indicates that the flow pattern in tank corners steers the incoming water in the negative x-direction, Figure 30. The red marking in Figure 30 represents the window of the flocculation unit available for measurements and section A-A represents the section where the experimental flow pattern was created. An animation through time for the numerical model would have been interesting to see to have a good view of how the flow pattern changes in this window.

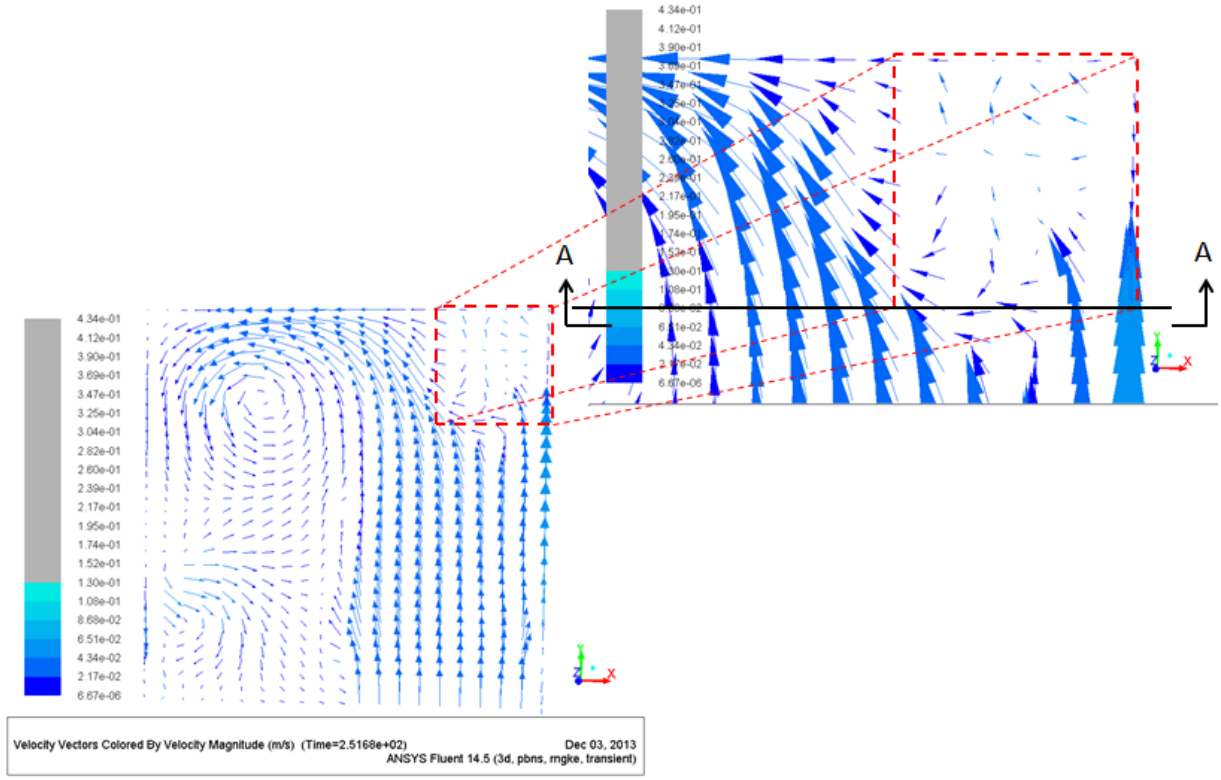

Figure 30. Top view of flow pattern in section Z= 3600 mm. Velocity vectors in the negative x and y direction can be seen in the measurement area.

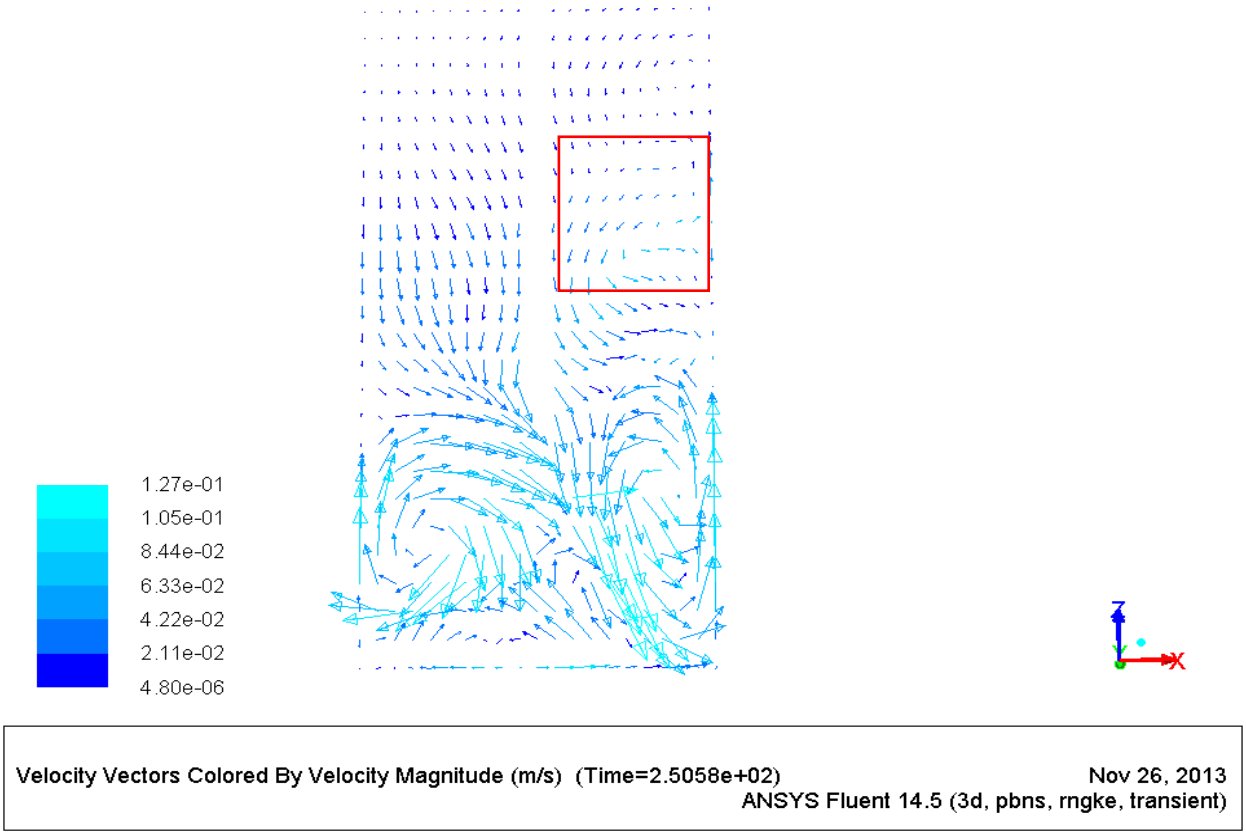

Figure 31. Sectional view of flow pattern in section Y= 1225 mm. Inlet location in relation to the section is marked with a rectangle (red).

In the section Y= 1225 mm it can be seen that only the lower parts in the tank are affected by the impeller motion, Figure 31. The velocity of the water flowing upwards along the walls in tank mid can be seen to be suppressed by the water being sucked into the impeller region in greater extent since the impeller blades are in more proximity to walls in tank mid. The velocity field in the unit will be dependent on the position of the impeller. In line with the impeller manufacturer Sulzer the numerical model show that the pitch-blade impeller pumps the water in the downward direction to later turn in the upward direction in the flocculation unit.

A diagonal section through the flocculation unit show that the water flows higher up in the unit. As can be seen in Figure 32 the water flows up to the level of the inlet and later flows down in a loop shape. It can be observed in Figure 32 the water seems to flow higher up in the unit in tank corners. Figure 32 is viewed in the direction of the resultant of the x and y axis.

The velocity gradients are highest below the impeller as could be suspected since the impeller pumps the water in the downward direction, Figure 33. Velocity is also high along tank walls since the main route for the water travelling upwards in the unit is along the walls. Just above the impeller high velocity gradient can also be seen this because the water is constantly being sucked down to the impeller region.

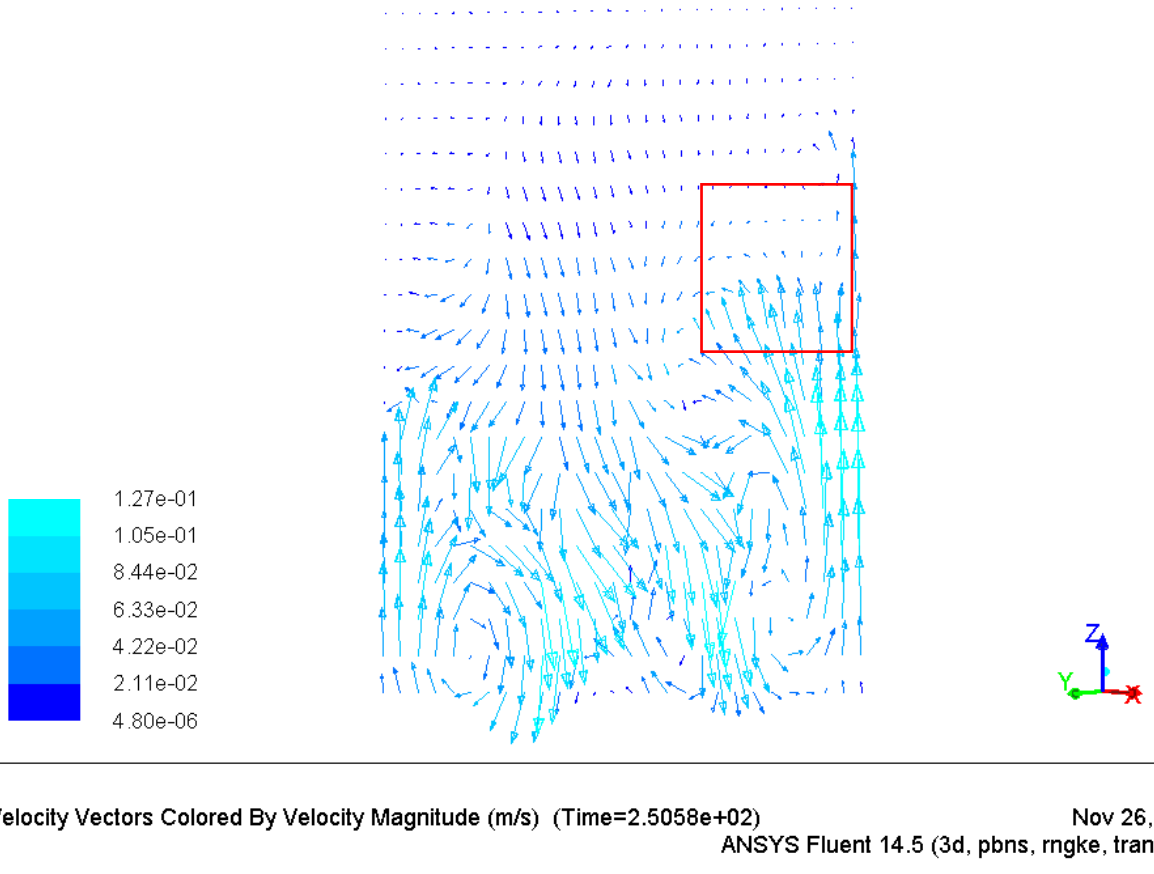

Figure 32. Sectional view of flow pattern in a diagonal section through the unit. The red marking represent the extents of the inlet in this section.

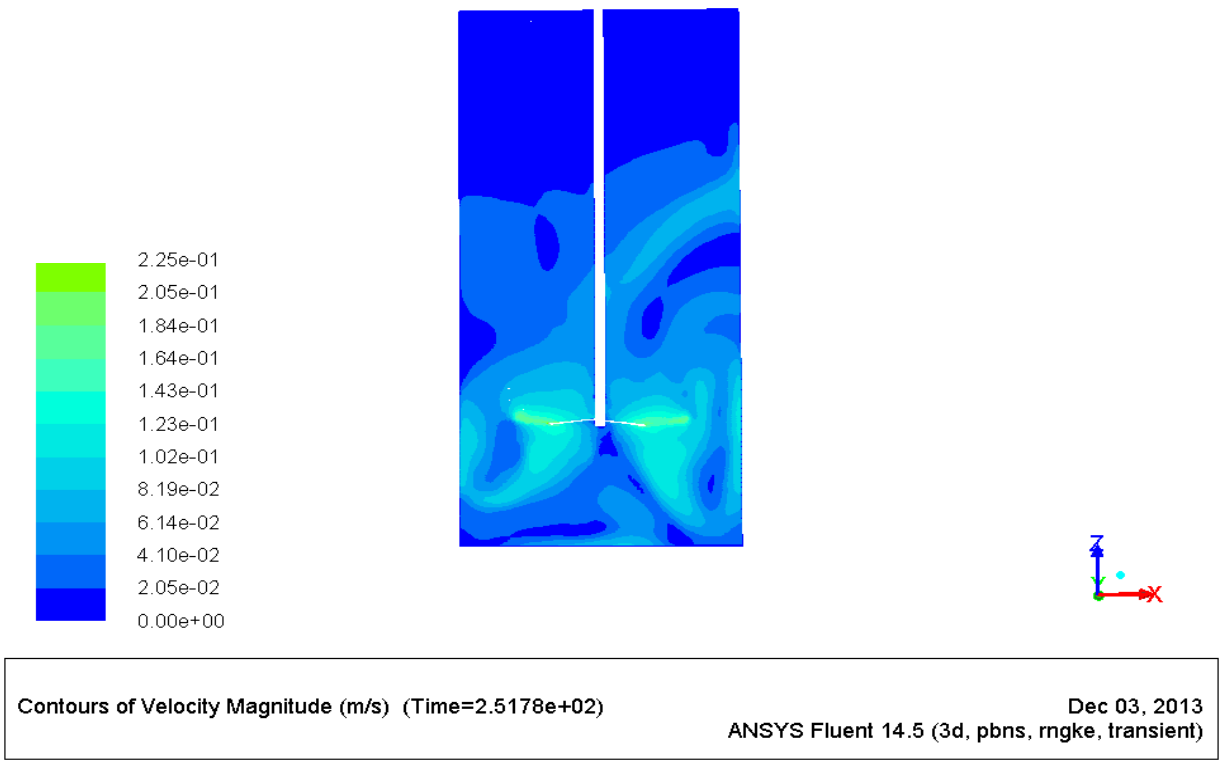

Figure 33. Sectional view of velocity magnitude contour in section Y= 1225 mm.

Comparison between experimentally derived flow pattern and numerical flow pattern in measurements B1211-B1217 will be made. The x-velocity direction derived experimentally corresponded to the numerically modelled for points B1211-B1217. The velocities were predominantly in the positive x-direction, Figure 16 and 34. The numerical model also predicted the negative x-direction for point B1214 that could be seen from the experimental measurements. The x-direction for points close to the surface showed however a negative x-velocity direction. This deviation in x-velocity direction in the uppermost points can be the result of that no surface model have been used and the fact that the water surface was modelled as being a wall. The z-velocity direction from the experimental measurements showed that the z-velocity direction should mainly be in the positive z-direction for points B1211-B1217. The numerical model showed the z-velocity to be in the negative z-direction. However since the z-velocities in the points are highly dependent on impeller location and time it would have been interesting to see an animation through time.

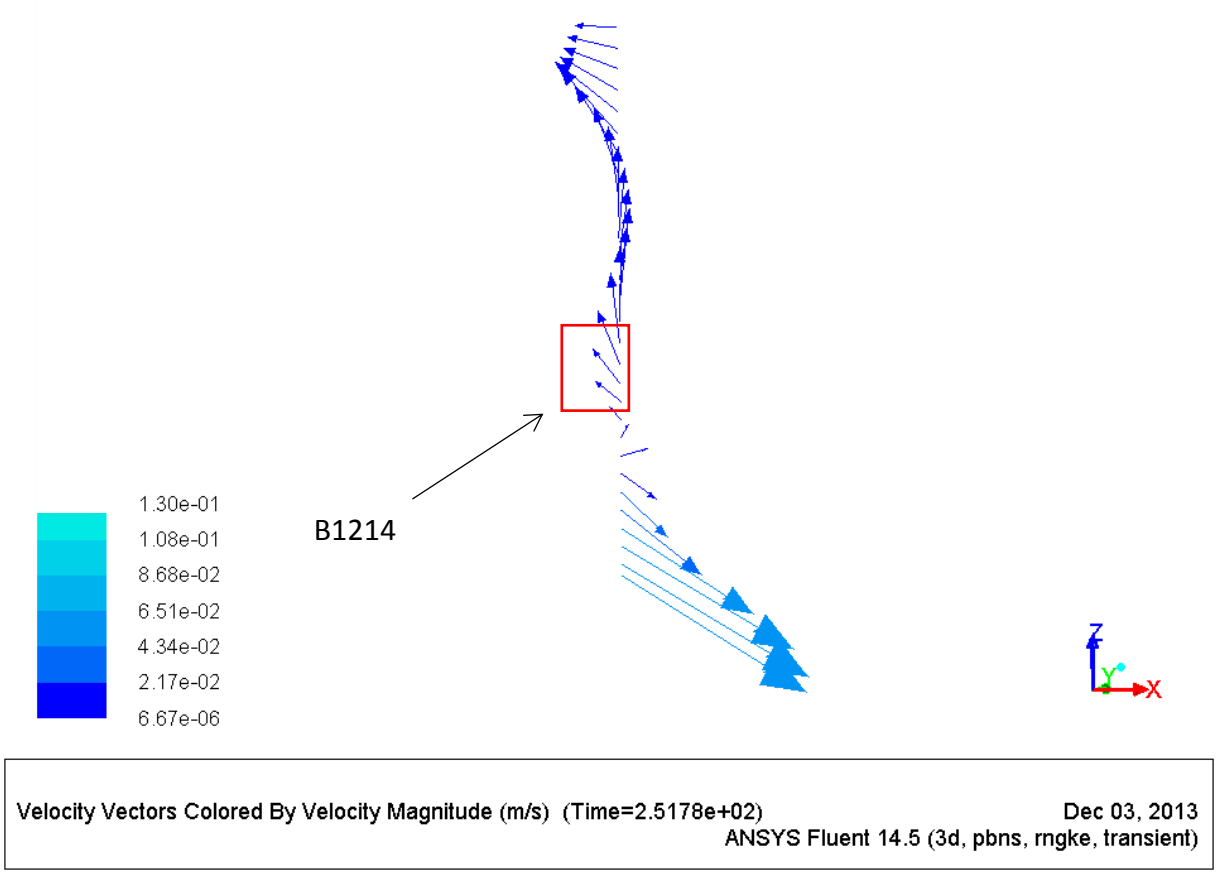

Figure 34. Flow pattern for points B1211-B1217 from the numerical model.

8. Concluding discussion

The flow division calculation with the propeller type current meter gave an inlet flow Q1 of 117 l/s compared to the treatment plant's assessment of flow Q1 being 200 l/s. Flow Q2 became 93 l/s. With the ADV instrument the inlet flow to flocculation unit number 1 was estimated to be 28 l/s. If one assumes that the same flow enters the other three remaining flocculation lines as well the flow to the old flocculation section would be 112 l/s. If one applies the ratios 30% and 70% to the estimated value of 112 l/s the flow Q1 would be 160 l/s. It is roughly said that the daily water consumption per person and day is 180 l. Överby drinking water treatment plant (DWTP) provides fresh drinking water to 49 000 inhabitants this would lead to a needed production of 9000 m^3 of water per day. A flow Q1 of 117 l/s would lead to a production of roughly 10 000 m^3/day and it does not sound reasonable since also industries can be connected to the municipal drinking water system. A flow Q1 of instead 160 l/s would lead to a production of drinking water of around 13 000 m^3/day which sounds more reasonable. However measurement with the ADV instrument for flow division instead of the propeller type current meter would be a better a better option. In Table 7 the expected, measured, and more reasonable flows for flow division can be viewed.

Table 7. Table on expected, measured, and probable flows from the flow division calculations.

	EXPECTED FLOWS (l/s)	MEASURED FLOWS (l/s)	PROBABLE FLOWS (l/s)
Q1	200	117	160
Q2	140	93	112
Q3	60	24	48

The experimental flow pattern showed good correlation to numerically obtained flow pattern. The x-velocity direction was predominantly in the positive direction from the experimental measurements which could also be shown from the numerical simulation. To evaluate the correlation between the measured mean z-velocity direction and numerically obtained z-velocity direction a transient animation would be needed. The z-velocity direction is highly dependent on time period and location of the impeller blades. The measurement point B1214 which showed deviating x-velocity direction from the experimental data could be also shown from the numerical model. The reason for this deviating x-velocity direction is believed to be related to the flow pattern generated by the impeller in these sections. Swirl motions could be seen at some sections in the flocculation unit these regions are believed to be turbulent and enhancing momentum transfer and can be seen as areas where flocs are more likely to grow in size. If the velocity shear rate is very high the flocs will instead break. The overall flow pattern in the flocculation unit is similar as the flow pattern described by the impeller manufacturer.

The numerical model made in this master thesis is a 3D model. A 2D model would perhaps have been a more economical approach with the limited computer power that was available. The numerical model is sufficient for estimating the global flow pattern but it can be improved. For increased accuracy, mesh refinement should be performed and perhaps also a surface model can be applied to the water surface in the unit. A solution animation can be performed, preferably, an animation with particle tracking to better visualize the flocculation hydrodynamics. To take it a step further would be to implement a population balance model in the CFD simulation to simulate the floc growth and floc breakage in the unit.

9. Conclusions

The flow in the flocculation unit and the flow division between the old and the new section have been measured using an ADV and a propeller type current meter. Generally, the ADV probe is believed to have given more reliable results in comparison to the propeller type current meter. All measurements carried out are, however, limited since each measure was carried out individually.

The flow division between the old and the new section is estimated to

- Q1= 160 l/s (total inflow)
- Q2= 112 l/s (flow to old flocculation section)
- Q3= 48 l/s (flow to new flocculation section)

Despite many difficulties converging the numerical model and limited time and computer resources available to refine the mesh, the results demonstrate that it is a promising approach to model the flow in the flocculation unit using CFD. The estimated flow pattern correlates well with the description of the intended flow pattern given by the impeller manufacturer Sulzer.

References

Andersson, B., Andersson, R., Håkansson, L., Mortensen, M., Sudiyo, R., Van Wachem, B. (2011). *Computational fluid dynamics for emgineers 9th ed*. Cambridge university press.

Ansys (2013). *Workbench user guide v14.5*. Ansys inc ISO 9001:2008.

Betancourt, W.Q., Rose, J.B. (2004). *Drinking water treatment processes for removal of Cryptosporidium and Giardia*. East Lansing, Michigan. Elseiver: Veterinary Parasitology 126 (2004) 219-234.

Bouyer, D., Line, A., Cockx, A., Do-Quang, Z. (2001). *Experimental analysis of floc size distribution and hydrodynamics in a jar-test*. Chemical Engineering Research and Design 79 (8) , pp. 1017-1024.

Bridgeman, J., Jefferson, B., Parson, S.A. (2009). The development and application of CFD models for water treatment flocculators. Elseiver: Advances in Engineering Software 41 (2010) 99–109.

Chanson, H., Trevethan, M., Aoki, S-I. (2008). *Acoustic Doppler velocimetry (ADV) in small estuary: Field experience and signal post-processing*. Elseiver: Flow Measurement and Instrumentation, Volume 19, Issue 5, October 2008, Pages 307-313.

Coufort, C., Bouyer, D., Liné, A. (2004). *Flocculation related to local hydrodynamics in a Taylor-Couette.* Elseiver: Chemical Engineering Science, Volume 60, Issues 8–9, April–May 2005, Pages 2179-2192.

Coufort, C., Bouyer, D., Liné, A., Haut, B., (2006). *Modelling of flocculation using a population balance equation*. Elseiver: Chemical Engineering and Processing 46 (2007) 1264–1273.

Crittenden, J.C., Trussel, R.R., Hand, D.W., Howe, K.J., Tchobanoglous, G., Borchardt, J.H., (2012). *MWH's Water Treatment- Principles and Design third edition.* Hoboken, New Jersey: John Wiley &Sons, Inc.Dewan, A. (2011). *Tackling turbulent flows in engineering*. Berlin-Heidelberg: Springer-verlag.

Edzwald, J.K. (1993). *Coagulation in drinking water treatment: Particles, organics and coagulants*. Water science and technology vol. 27 no.11, pp 21-35.

Hirsch, C., (2007). *Numerical computation of internal and external flows: Introduction to the fundamentals of CFD 2nd edition*. Elseiver: The Fundamentals of Computational Fluid Dynamics 2007, Pages 1–20, I–V.

Jesson, M., Sterling, M., Bridgeman, J. (2012). *Despiking velocity time-series – optimization through the combination of spike detection and replacement methods*. Elseiver: Flow Measurement and Instrumentation, Volume 30, April 2013, Pages 45-51.

Jiang, J.Q., Graham, N.J.D. (1998). *Pre-polymerised inorganic coagulants and phosphorus removal by coagulation- a review*. London. Environmental and water resource engineering, Department of Civil Engineering, Imperial College of science.

Jiyuan, T., Guan-Heng, Y., Chaoqun, L. (2012). *Computational fluid dynamics: A practical approach second ed.* Butterworth-Heinemann.

Joseph, A. (2014). *Measuring ocean currents: tools, technologies, and data.* Elseiver: Measuring Ocean Currents, 2014, Pages 51-92.

Kilander, J., Blomström, S., Rasmuson, A. (2007). *Scale-up behaviour in stirred square flocculation tanks.* Chemical Engineering Science 62 (6) , pp. 1606-1618.

Li, T., Zhu, Z., Wang, D., Yao, C., Tang, H. (2006). *Characterization of floc size, strength and structure under various coagulation mechanisms.* Elseiver: Powder Technology, Volume 168, Issue 2, 11 October 2006, Pages 104-110.

Lundh, M., Jönsson, L. (2002). *Performance evaluation of the Acoustical Doppler Velocimeter in water with high contents of micro-bubbles*. Journal of hydraulic research.

Matilainen, A., Vepsäläinen, M., Sillanpää, M., (2010). *Natural organic matter removal by coagulation during drinking water treatment: A review*. Advances in Colloid and Interface Science 159 (2) , pp. 189-197.

Peltier, Y., Rivièrea, N., Proust, S., Mignot, E., Paquier, A., Shionoc, K. (2013). *Estimation of the error on the mean velocity and on the Reynolds stress due to a misoriented ADV probe in the horizontal plane: Case study of experiments in a compound open-channel.* Elseiver: Flow Measurement and Instrumentation, Volume 34, December 2013, Pages 34-41.

Samaras, K., Zouboulis, A., Karapantsios, T., Kostoglou, M., (2010). *A CFD-based simulation study of a large scale flocculation tank for poTable water treatment.* Elseiver: Chemical Engineering Journal, Volume 162, Issue 1, 1 August 2010, Pages 208-216.

Somasundaran, P., Runkana, V. (2003). *Modelling flocculation of colloidal mineral suspensions using population balances.* Elseiver: International Journal of Mineral Processing, Volume 72, Issues 1–4, 29 September 2003.

Trollhättan energi. (2013). *Bakgrund till vattenverket.* Trollhättan energi.

Xiao, F., Lam, K.M., Li, X.Y., Zhong, R.S., Zhang, X.H. (2011). *PIV characterisation of flocculation dynamics and floc structure in water*. Colloids and Surfaces A: Physicochemical and Engineering Aspects 379 (1-3) , pp. 27-35.

Xu, W., Gaoa, B., Wanga, Y., Yuea, Q., Renb, H. (2012). *Effect of second coagulant addition on coagulation efficiency, floc properties and residual Al for humic acid treatment by Al13 polymer and polyaluminum chloride(PACl)*. Elseiver: Journal of Hazardous Materials, Volumes 215–216, 15 May 2012, Pages 129-137.

Zhao, Y.X., Gao, B.Y., Zhang, G.Z, Phuntsho, S., Wang, Y., Yue, Q.Y., Li, Q., Shon, H.K., (2013). *Comparative study of floc characteristics with titanium tetrachloride against conventional coagulants: Effect of coagulant dose, solution pH, shear force and break-up period.* Elseiver: Chemical Engineering Journal, Volume 233, November 2013, Pages 70-79.